This is an open access article published under an ACS AuthorChoice License, which permits copying and redistribution of the article or any adaptations for non-commercial purposes.

Chemical Research in Toxicology

Perspective

pubs.acs.org/crt

Systems Toxicology Assessment of the Biological Impact of a Candidate Modified Risk Tobacco Product on Human Organotypic Oral Epithelial Cultures

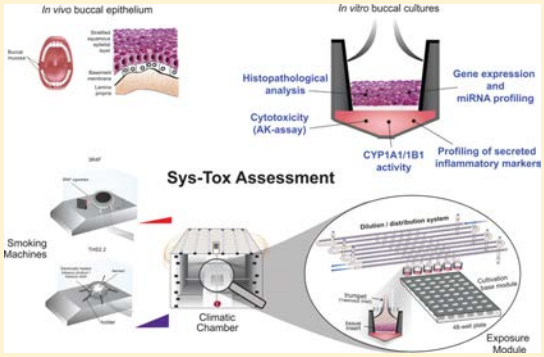
Filippo Zanetti,[†] Alain Sewer,[†] Carole Mathis,[†] Anita R. Iskandar,[†] Radina Kostadinova,[†] Walter K. Schlage,[‡] Patrice Leroy,[†] Shoaib Majeed,[†] Emmanuel Guedj,[†] Keyur Trivedi,[†] Florian Martin,[†] Ashraf Elamin,[†] Céline Merg,[†] Nikolai V. Ivanov,[†] Stefan Frentzel,[†] Manuel C. Peitsch,[†] and Julia Hoeng*[,†]

[†]Philip Morris International Research and Development, Quai Jeanrenaud 5, 2000 Neuchâtel, Switzerland

[‡]Biology Consultant, Max-Baermann-Str. 21, 51429 Bergisch Gladbach, Germany

Supporting Information

ABSTRACT: Cigarette smoke (CS) has been reported to increase predisposition to oral cancer and is also recognized as a risk factor for many conditions including periodontal diseases, gingivitis, and other benign mucosal disorders. Smoking cessation remains the most effective approach for minimizing the risk of smoking-related diseases. However, reduction of harmful constituents by heating rather than combusting tobacco, without modifying the amount of nicotine, is a promising new paradigm in harm reduction. In this study, we compared effects of exposure to aerosol derived from a candidate modified risk tobacco product, the tobacco heating system (THS) 2.2, with those of CS generated from the 3R4F reference cigarette. Human organotypic oral epithelial tissue cultures (EpiOral, MatTek Corporation) were exposed for 28 min to 3R4F CS or THS2.2 aerosol, both diluted with air to comparable nicotine concentrations (0.32 or 0.51 mg nicotine/L aerosol/CS for 3R4F and 0.31 or 0.46 mg/L for THS2.2). We also tested one higher concentration (1.09 mg/L) of THS2.2. A systems toxicology approach was employed combining cellular assays (i.e., cytotoxicity and cytochrome P450 activity assays), comprehensive molecular investigations of the buccal epithelial transcriptome (mRNA and miRNA) by means of computational network biology, measurements of secreted proinflammatory markers, and histopathological analysis. We observed that the impact of 3R4F CS was greater than THS2.2 aerosol in terms of cytotoxicity, morphological tissue alterations, and secretion of inflammatory mediators. Analysis of the transcriptomic changes in the exposed oral cultures revealed significant perturbations in various network models such as apoptosis, necroptosis, senescence, xenobiotic metabolism, oxidative stress, and nuclear factor (erythroid-derived 2)-like 2 (NFE2L2) signaling. The stress responses following THS2.2 aerosol exposure were markedly decreased, and the exposed cultures recovered more completely compared with those exposed to 3R4F CS.



CONTENTS

Introduction 1253
Materials and Methods 1254
- Organotypic Culture Models 1254
- Test and Reference Items 1254
- Vitrocell 3R4F Smoke and THS2.2 Aerosol Exposure 1254
- Nicotine Determination and Standardization in 3R4F Smoke and THS2.2 Aerosol 1254
- Deposited Carbonyls in the Vitrocell Base Module Following 3R4F Smoke and THS2.2 Aerosol Exposures 1255
- AK-Based Cytotoxicity Assay 1255
- Histological Analysis 1255
- Cytochrome P450 (CYP) Activity 1255
- Luminex-Based Measurement of Secreted Analytes 1255
- Transcriptomics and Computational Evaluation of mRNA and miRNA 1255
- Statistical and Reproducibility Analysis 1256
  - Cytotoxicity, CYP Activity, and Proinflammatory Mediators 1256
  - Gene/miRNA Expression 1256

Results 1256
- Selection of 3R4F CS and THS2.2 Aerosol Concentrations 1256
- Cytotoxicity and Tissue Morphology 1256
- Alterations of CYP1A1/CYP1B1 Activity 1257

Received: May 17, 2016
Published: July 12, 2016

 © 2016 American Chemical Society

DOI: 10.1021/acs.chemrestox.6b00174
Chem. Res. Toxicol. 2016, 29, 1252−1269

Profiles of Secreted Proinflammatory Mediators 1258
Exposure Impact on mRNA Profiles 1258
Mechanistic Networks and Gene Pathways 1258
Exposure Impact on Specific Marker Genes 1260
Exposure Impact on miRNA Profiles 1261
Correlation of the Outcomes Across the Experimental Repetitions 1262
Discussion 1262
Conclusions 1264
Associated Content 1264
Supporting Information 1264
Author Information 1264
Corresponding Author 1264
Funding 1264
Notes 1265
Biographies 1265
Acknowledgments 1266
Abbreviations 1266
References 1266

INTRODUCTION

The function of the oral mucosa is to protect underlying tissues and organs against physical, mechanical, chemical, and microbial insult.[1] Exposure to ingested toxicants can alter the structure of the oral epithelia, leading to either adaptive/reactive or pathological changes.[2−4] Exposure to cigarette smoke (CS) is a recognized risk factor for the development of oral diseases. Besides its well-known effects of increasing predisposition to oral cancer,[5−7] CS has been linked to benign mucosal conditions, including periodontal diseases, gingivitis, and other disorders.[8−11] Because CS enters an organism through the mouth via the oral cavity, the proper functioning of the oral epithelium is important as a first defense and requires a balance among proliferation, differentiation, and desquamation or death of its cells.[12,13] Though exposure to CS did not affect the cell cycle in oral keratinocytes, it altered the number of cells with early and late apoptotic features, indicating effects on the oral epithelial biology.[13] Changes in cellular differentiation were detected as early as 3 h after CS exposure in basal and suprabasal layers of explanted oral epithelium *in vitro*, though no effects on intercellular adhesion and barrier functions were observed.[12] Changes in gene expression were also observed in oral epithelia from smokers, though in some cases accompanied by noticeable histological or phenotypic effects.[14−16] Often, however, cytologic, genomic, and transcriptomic changes in oral mucosa were associated with oral inflammatory diseases (e.g., periodontitis) or with preneoplasia and cancers of the aero-digestive tract.[17−22] We recently reported that CS exposure induced secretion of proinflammatory mediators and altered gene expression profiles, in particular by impacting gene networks related to xenobiotic metabolism and cellular stress, in reconstituted human organotypic oral (buccal and gingival) epithelial models. Moreover, our transcriptomics results were similar to reported findings in buccal mucosa biopsies from smokers and nonsmokers.[23]

Organotypic cultures are a valuable tool to study effects of aerosol exposure on target tissues, enabling exposure at the air−liquid interface (ALI). These cultures retain the 3D structure and functional polarization typical of native epithelium, and are available from human donors of various ethnic backgrounds in high throughput formats.[24] Moreover, they show response characteristics similar to those of *in vivo* tissues;[23,25−27] they are therefore regarded as suitable, relevant models for investigating the biology, pathology, and immunology of the oral mucosa.[26−35] In particular, the EpiOral (MatTek Corporation) mucosal model was used to measure cell viability and cytokine release in response to oral care excipients and prototype formulations. This differentiated model has active antimicrobial properties, expression of hBD1 and hBD3 peptides in response to TNF-α, and an intact surface barrier for protection against oral bacteria.[25] Several studies demonstrated the suitability of organotypic oral cell cultures for cancer-related research.[27,30,33,36,37] Organotypic oral cell cultures were used to assess cellular response to mouthwashes and dental materials, including bonding adhesives, orthodontic wires, and nickel, as well as in models of gingivitis and periodontitis to evaluate tissue invasion by *Porphyromonas gingivalis*[29,34] and *Streptococcus salivaris*, demonstrating inflammatory marker release.[31,32]

A recent review by Manuppello and Sullivan outlines technological advances in *in vitro* assessment of tobacco products.[38] These include the use of reconstituted human lung organotypic cultures that enable exposure at the ALI to test the toxicity of tobacco smoke, E-cigarette aerosols, constituents, and particulates. Organotypic buccal and gingival epithelial culture models were used to assess effects of exposure to airborne environmental toxicants such as CS, facilitating mechanistic investigations, environmental studies, and product testing.[23]

Regulatory and chemical safety testing are major drivers for developing experimental systems that are alternatives to animal models, in line with the principle of the 3Rs (replacement, reduction, and refinement).[39] With the advent of 21st century toxicology approaches, there has been tremendous interest in bringing such methodologies into regulatory use, with debates ongoing about their applicability.[40] Several approaches aimed at replacing animals with organotypic cultures have already been used in pharmaceutical research to detect potential toxicity in the heart, lungs, and liver.[41−43] Knudsen et al., in a paper describing their "Future ToxII" visionary outlook, suggested that 3D organotypic culture models, along with human "organ-on-chip" microscale physiological systems, have the potential to change the current landscape of toxicological risk assessment.[44]

Smoking cessation is the primary way to avoid harmful effects of CS. However, switching to a reduced risk product, termed "modified risk tobacco product" (MRTP), is a potential alternative for lowering the risk of smoking related diseases.[45,46]

We here report the assessment of the biological impacts of exposure to aerosol from a candidate MRTP, the Tobacco Heating System (THS) 2.2, compared with conventional smoke derived from 3R4F reference cigarettes, in organotypic oral (buccal, EpiOral provided by MatTek) epithelial cultures. THS2.2 is based on a heat-not-burn technology that heats, instead of burning, specifically designed tobacco sticks (Philip Morris International R&D). A comparative analysis between THS2.2 aerosol and 3R4F CS were performed before.[49,50]

EpiOral cultures, were exposed to 3R4F CS or THS2.2 aerosol for 28 min, at comparable nicotine concentrations plus one higher for THS2.2. Tissue response was assessed with a systems toxicology approach, combining cellular assays, comprehensive molecular investigations of the buccal epithelial transcriptome (mRNA and miRNA) based on computational network biology, measurements of secreted proinflammatory markers and histopathological analyses.

This study indicates that exposure to THS2.2 aerosol, compared with 3R4F CS at the matching nicotine concentrations, was not cytotoxic and caused significantly reduced effects on the histopathology and secretion of inflammatory mediators together with the fastest recovery of the gene expression changes.

DOI: 10.1021/acs.chemrestox.6b00174
Chem. Res. Toxicol. 2016, 29, 1252−1269

MATERIALS AND METHODS

Organotypic Culture Models. The organotypic human oral epithelial culture model EpiOral (ORL-200) was purchased from MatTek (Ashland, MA, USA). Undifferentiated epithelial cells were used to construct the EpiOral models. The oral epithelial cells used throughout the study were isolated from the same donor, a healthy nonsmoking man, age 46 years. The cells were cultured at the ALI in 0.7 mL of medium in 24 well plates with Transwell inserts (6.5 mm diameter, 0.4 μm pore size, Corning, Tewksbury, MA, USA and Greiner Bio-One, Monroe, NC, USA).

Upon delivery, the oral cultures had been grown for 14 days after seeding. The organotypic cultures were maintained in-house at 37 °C for 3 days before exposure experiments, to complete the differentiation at the ALI, with fresh medium (ORL-200 DM4A, MatTek) according to the supplier's instructions. After differentiation, the organotypic cultures were incubated in maintenance medium (ORL-200-MM, MatTek) and the medium changed every 48 h as recommended by the supplier. Both media used in the study (differentiation and maintenance) were produced by MatTek, and their compositions have not been disclosed to the public. At 3−4 days after arrival, organotypic cultures were exposed to 3R4F CS or THS2.2 aerosol according to each experimental design. After the exposures, the cultures were maintained for up to 48 h without changing the medium; for the adenylate kinase (AK) assay and the collection of proinflammatory markers, the medium was kept unchanged until 72 h postexposure. Integrity of the cultures was assessed microscopically throughout the study.

Test and Reference Items. Two items were used for exposures administered in this study: 3R4F cigarettes (reference item) (University of Kentucky, Kentucky Tobacco Research and Development Center, www.ca.uky.edu/refcig) and THS2.2 sticks (test item) (Philip Morris international R&D, Neuchatel, Switzerland). 3R4F cigarettes and THS2.2 sticks were conditioned for at least 48 h and up to 21 d at 22 ± 1 °C with a relative humidity of 60 ± 3%, according to ISO standard 3402.[47]

Vitrocell 3R4F Smoke and THS2.2 Aerosol Exposure. Four experimental repetitions and experiments associated with a dose range assessment (DRA) phase were performed over a period of 4 months. For each repetition, 3 independent exposures (28 min each) were performed.

For each exposure run, 10 3R4F cigarettes were smoked for 10−11 puffs each to a standard butt length (approximately 35 mm) and 10 THS2.2 sticks were aerosolized up to 12 puffs each. These conditions were in accordance with the Health Canada smoking regimen, with 55 mL puff over 2 s, twice per min with an 8 s pump exhaust time.[48]

CS was generated from 3R4F reference cigarettes, and the test aerosol was generated from THS2.2, each inserted into a dedicated 30-port carousel smoking machine SM 2000 (Philip Morris International, NE, Switzerland). These smoking machines are referred to as SM 2000-3R4F and SM 2000-THS2.2 for 3R4F and THS2.2, respectively. CS or THS2.2 aerosol was conducted to the Vitrocell 24/48 dilution and exposure system (Vitrocell 24/48 for 24 well sized inserts) (Vitrocell Systems GmbH, Waldkirch, Germany). The inserts were placed in the climatic chamber of the Vitrocell exposure system and directly exposed to the diluted 3R4F CS or THS2.2 aerosol. Dilution was achieved with filtered air conditioned to 60% relative humidity, in the dilution and distribution systems, as illustrated in Figure S1.

A pair design was implemented where the samples (to 3R4F CS or THS2.2 aerosol) were exposed together with their corresponding air controls during each exposure run (Figure S1).

Various end points were measured for each group (Figure 1) (for more details, see Table S1).

Nicotine Determination and Standardization in 3R4F Smoke and THS2.2 Aerosol. The nicotine concentrations were determined in CS/aerosol samples taken directly from the dilution system on Extrelut 3NT columns (Merck, Zug, Switzerland) soaked with 2 mL of 0.5 M H_2SO_4 and measured by gas chromatography as described in detail elsewhere.[49]

To determine target concentrations of nicotine in the smoke or aerosol, various dilutions were applied to the organotypic culture models.

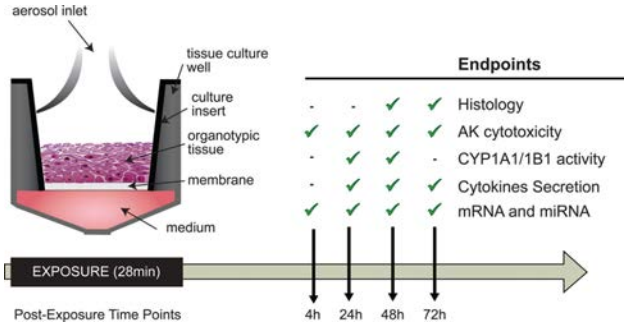


Figure 1. Schematic representation of the experimental design. The figure illustrates the tissue culture well where the inset holding the organotypic culture is placed. The culture is separated from the basal medium with a permeable membrane. The insert is exposed for 28 min to 3R4F CS or THS2.2 aerosol. Different end points are analyzed at the indicated postexposure time points as represented.

Prior to starting the experimental repetitions, a dose range finding (DRF) experiment was performed to find the maximum tolerable concentration of 3R4F CS. We used nicotine as the internal reference compound to compare and normalize the concentrations of THS2.2 aerosol to those of 3R4F CS. We selected 2 3R4F CS and THS2.2 aerosol concentrations, each pair matched for nicotine concentrations, for the comparative analysis. In addition, we added another group to test a higher THS2.2 aerosol exposure. Table 1 shows the target nicotine concentrations established during the DRF compared with the actual average concentrations achieved during the 4 experimental repetitions by diluting 3R4F CS and THS2.2 aerosols. By diluting 3R4F CS with air at 15%, we obtained an average concentration of 0.32 mg nicotine/L. The nicotine concentration matching this dilution was the lowest THS2.2 aerosol concentration (25%, giving 0.31 mg/L). Higher dose comparable nicotine concentrations were obtained by diluting the 3R4F CS to 24% (0.51 mg/L) and

Table 1. Target and Actual Nicotine Concentrations in 3R4F CS and THS2.2 Aerosol[a]

group	study phase		average trapping
3R4F low concentration	DRF	smoke concentration (%)	20
		target nicotine (mg/L)	0.3
	experimental repetition	smoke concentration (%)	15
		actual nicotine (mg/L)	0.32 ± 0.008 (N = 12)
3R4F high concentration	DRF	smoke concentration (%)	30
		target nicotine (mg/L)	0.5
	experimental repetition	smoke concentration (%)	24
		actual nicotine (mg/L)	0.51 ± 0.010 (N = 12)
THS2.2 low concentration	DRF	smoke concentration (%)	30
		target nicotine (mg/L)	0.3
	experimental repetition	aerosol concentration (%)	25
		actual nicotine (mg/L)	0.31 ± 0.008 (N = 14)
THS2.2 medium concentration	DRF	smoke concentration (%)	45
		target nicotine (mg/L)	0.5
	experimental repetition	aerosol concentration (%)	32
		actual nicotine (mg/L)	0.46 ± 0.020 (N = 14)
THS2.2 high concentration	DRF	smoke concentration (%)	80
		target nicotine (mg/L)	1.1
	experimental repetition	aerosol concentration (%)	69
		actual nicotine (mg/L)	1.09 ± 0.025 (N = 14)

[a]Nicotine concentrations are expressed as the means ± SEM. N, number of samples trapped in the EXtrelut 3NT columns.

DOI: 10.1021/acs.chemrestox.6b00174
Chem. Res. Toxicol. 2016, 29, 1252−1269

THS2.2 aerosol to 32% (0.46 mg/L). The highest THS2.2 concentration chosen (69%, giving 1.09 mg/L) had almost twice the nicotine concentration of the higher 3R4F CS concentration (0.51 mg/L). For the nicotine concentrations utilized during the DRA phase, see Table S2.

Deposited Carbonyls in the Vitrocell Base Module Following 3R4F Smoke and THS2.2 Aerosol Exposures. Carbonyls were measured in phosphate buffered saline (PBS) following a 28 min exposure to smoke or aerosol, 10 sticks per item, using the smoking protocol described above. Briefly, before exposure, each row in the cultivation base module of the Vitrocell 24/48 was filled with 18.5 mL of PBS. Following exposure, a 1.2 mL aliquot of each PBS-exposed sample (per row) was collected and analyzed by high-performance liquid chromatography (HPLC) coupled with a tandem MS (HPLC-MS/MS), as previously reported,[49] to measure acetaldehyde, acetone, acrolein, methyl ethyl ketone, crotonaldehyde, and propionaldehyde (Figure S2).

AK-Based Cytotoxicity Assay. AK release was used as a marker for cytotoxicity. Cell viability was assessed in the basolateral medium of CS- and aerosol-exposed organotypic cultures using an AK assay kit (ToxiLight bioassay kit; Lonza, Rockland, MA, USA) according to the manufacturer's recommendations. The luminescence signals were measured with a FluoStar Omega reader (BMG Labtech GmbH, Ortenberg, Germany). Each value of AK was calculated by normalizing the average of the positive control (cultures treated with 1% Triton X-100 for 24 h at the basolateral side) and the negative control (untreated cultures). 1% Triton X-100 treatment was considered to completely lyse the cells (100% cytotoxicity).

Histological Analysis. The organotypic cultures were washed 3 times with PBS and fixed for 2 h in 4% (w/v) paraformaldehyde (PFA). They were washed again at room temperature, both apically and basally, 3 times with PBS once fixation was completed. After this process, fixed cultures were separated from the insets by detaching the membrane from the plastic with a forceps and were bisected through the middle prior to processing with a Leica ASP300S tissue processor (Leica Biosystem Nussloch GmbH, Nussloch, Germany). After embedding samples into paraffin blocks, 5 μm sections were cut with a microtome. These sections were mounted on glass slides and transferred to the automated slide stainer, Leica ST5020 (Leica Biosystem Nussloch GmbH). Sections were stained with a standard hematoxylin (Merck Millipore, Schaffhausen, Switzerland) and eosin (Sigma-Aldrich, St. Louis, MO, USA) (H&E) procedure.

For immunohistochemical staining, slides were incubated at 60 °C for a minimum of 30 min and then transferred to the Leica Bond-Max autostainer for immunohistochemistry using Leica Bond Polymer Refine Detection Kit (Leica # DS9800). The slides were treated with ethylenediaminetetraacetic acid (EDTA), incubated with an E-cadherin antibody (Leica Biosystem PA0387, undiluted) and counterstained with hematoxylin.

Three slides per condition or experimental replicate were stained. Digital images of each slide were generated using the Hamamatsu NanoZoomer slide scanner (Hamamatsu Photonics, K.K., Japan), with images acquired at 20× magnification.

Cytochrome P450 (CYP) Activity. The combined activity of the cytochrome P450 (CYP) isozymes 1A1 and 1B1 was measured at 24 and 48 h postexposure in the basolateral medium of the EpiOral cultures using the nonlytic P450-Glo assay (Promega, Madison, WI, USA) based on luminescence, according to the manufacturer's recommendations. Organotypic cultures were incubated for 24 h prior to sample collection in medium with luminogenic CYP-Glo substrate, luciferin-CEE, a substrate for both CYP1A1 and CYP1B1. Light was emitted upon addition of the luciferin detection reagent and quantified after 20 min of incubation at room temperature in a FluoStar Omega reader (BMG Labtech GmbH). As a positive control, organotypic cultures were treated with 30 nM 2,3,7,8-tetrachlorodibenzo-*p*-dioxin (TCDD), added to the basolateral medium 48 h before sample collection, and replenished after 24 h.

Luminex-Based Measurement of Secreted Analytes. The measurement of secreted proinflammatory mediators was performed, at each exposure time point indicated, by collecting 200 μL aliquots of the basolateral medium from EpiOral cultures. The profiling was done using Luminex xMAP technology (Luminex, Austin, TX, USA) with commercially available assay panels (EMD Millipore Corp., Schwalbach, Germany) to detect the following mediators: colony-stimulating factor (CSF)2, CSF3, interleukin (IL)6, chemokine (C-X-C motif) ligand (CXCL)8, CXCL10, matrix metalloproteinase (MMP)1, IL1α, IL1β, transforming growth factor alpha (TGFA), and vascular endothelial growth factor alpha (VEGFA). The assay was performed according to the manufacturer's instructions. Briefly, 25 μL of diluted or undiluted sample was used for each detection, and the analysis was conducted on a Luminex, 200 or FLEXMAP 3D reader, equipped with the xPONENT software (Luminex, Austin, TX, USA). As a positive control, a set of triplicate samples was treated for 24 h with tumor necrosis factor (TNF)α and IL1β in the basolateral medium, each at a final concentration of 10 ng/mL. As a negative control to determine basal levels of the secreted mediators, a second set of triplicate samples was treated for 24 h with PBS in the basolateral medium. Whenever measured concentrations fell below the limit of quantitation, the concentrations were calculated by dividing the lower limit of detection by two.

Transcriptomics and Computational Evaluation of mRNA and miRNA. Total RNA was isolated and purified (Supporting Information, Methods: RNA and miRNA Purification). The resulting cocktail was hybridized into Affymetrix GeneChip HG U133 Plus 2.0 arrays to generate the CEL files containing the probe set intensities (Supporting Information, Methods: mRNA Microarray). These raw data underwent quality control before being transformed into the expression matrix used to calculate the gene differential expressions; all raw and normalized data were submitted to ArrayExpress repository (ID: E-MTAB-4742) (Supporting Information, Methods: Processing Raw CEL Files of the mRNA Microarray). To infer the biological effects of exposures from the mRNA differential expression data, we conducted a network-based systems biology approach,[50] complemented by a standard gene-set analysis (GSA). We used a collection of 28 biological network models containing literature-supported cause-and-effect relationships and hierarchically organized into families representing general biological processes (see Table 2): cell fate (CFA), cell proliferation

Table 2. List of Network Models Considered in the Study

no	abbreviated network family name	network name
1	CFA	apoptosis
2	CFA	autophagy
3	CFA	necroptosis
4	CFA	response to DNA damage
5	CFA	senescence
6	CPR	calcium
7	CPR	cell cycle
8	CPR	cell interaction
9	CPR	clock
10	CPR	epigenetics
11	CPR	growth factor
12	CPR	hedgehog
13	CPR	Hox
14	CPR	Jak STAT
15	CPR	Mapk
16	CPR	MTor
17	CPR	Notch
18	CPR	nuclear receptors
19	CPR	PGE2
20	CPR	Wnt
21	CST	endoplasmic reticulum stress
22	CST	hypoxic stress
23	CST	NFE2L2 signaling
24	CST	osmotic stress
25	CST	oxidative stress
26	CST	xenobiotic metabolism response
27	IPN	epithelial innate immune activation
28	IPN	tissue damage

DOI: 10.1021/acs.chemrestox.6b00174
Chem. Res. Toxicol. 2016, 29, 1252−1269

(CPR), cell stress (CST), and inflammatory processes network (IPN).[51] Network-level exposure effects were quantified as "Network Perturbation Amplitude" (NPA),[52] while the overall exposure impact was assessed by the "Biological Impact Factor" (BIF) (Supporting Information and Methods: Calculating Network Perturbation Amplitudes for Transcriptomics Data and Calculating Biological Impact Factors for Transcriptomics Data).[53] GSA was included as a widely used approach for interpreting gene differential expressions aiming at confirming and possibly complementing the NPA-based results (Supporting Information, Methods: Gene-Set Analysis of Transcriptomics Data).

Mature microRNAs (miRNAs) were isolated and purified (Supporting Information, Methods: RNA and miRNA Purification). The resulting cocktail was hybridized into Affymetrix GeneChip miRNA arrays (version 4.0) to generate the CEL files containing the probe set intensities (Supporting Information, Methods: miRNA Microarray). These raw data underwent quality control and several filtering steps before being transformed into the final expression matrix used to calculate the miRNA differential expressions (Supporting Information, Methods: Processing Raw CEL Files of the miRNA Microarray). These values were combined with the gene differential expressions to apply a gene-set-based over-representation analysis of the associated mRNA targets (Supporting Information, Methods: miRNA Functional Analysis).

Statistical and Reproducibility Analysis. Statistical analysis was performed using SAS software version 9.2 (SAS, Wallisellen, Switzerland) on data from AK assays, CYP activities, and luminex-based measurements of secreted mediators, while $R\bar{3}.1.2$ and Bioconductor 3.0 were used to perform gene/miRNA analyses.[54] Mean and standard error of the mean (SEM) values were reported unless otherwise specified. Comparisons of data from an exposed sample versus its air control (i.e., the paired-sample from the same exposure run) were performed using a paired t test, and the raw p-values obtained were reported. Before applying the paired t test to data from secreted mediator analyses (Luminex assay), the values were transformed using the natural log transformation. For the gene/miRNA analyses, the same comparisons were performed though using a moderated paired t test, and (Benjamini-Hochberg) adjusted p-values were considered.

Cytotoxicity, CYP Activity, and Proinflammatory Mediators. This study was designed to incorporate measurement errors, such as those introduced by organotypic culture batches and exposure runs, and was conducted with multiple experimental repetitions. To investigate the variability among experimental repetitions, the average was computed separately for each end point, treatment, and postexposure duration; then, the Spearman correlation was calculated between the average of the differences between the measurements of exposed and nonexposed samples computed for experimental repetitions 1 and 2 and versus the average computed for 3 and 4.

Gene/miRNA Expression. Reproducibility was estimated by correlating the fold-changes (exposed samples versus controls) across experimental repetitions. First, the gene/miRNA expression data from experiments 1 and 2 were combined, and the fold-changes were computed for each comparison and each gene/miRNA in the data set. The combined data from experiments 3 and 4 were in-turn used to compute the corresponding fold-changes. Correlation plots of the fold-changes for all genes/miRNA in the data set were then generated for each comparison.

RESULTS

Selection of 3R4F CS and THS2.2 Aerosol Concentrations. Prior to starting the main experiments, a DRF phase was performed to find the maximum tolerable dose (MTD) of 3R4F CS and THS2.2 aerosol. While no obvious effect on tissue-like morphology of the cultures was observed for any concentration (up to 80%) of THS2.2 aerosol tested (data not shown), 3R4F CS exposure showed detectable morphological damage beginning at 40% concentration, with nearly total disruption of tissue-like structure at 50%, thereby exceeding the MTD. Comparable effects were observed in cultures derived from two different donors (Figure S3). For the main experimental repetitions, we selected the 20 and 30% 3R4F CS concentrations (corresponding to target nicotine levels shown in Table 1) and the comparable concentrations of the THS2.2 aerosol, along with one higher THS2.2 aerosol concentration. This choice was made to allow the assessment of effects relevant to toxicity-related mechanisms associated with exposure, instead of effects reflecting morphological alterations associated only with severely damaged tissue.[55]

Cytotoxicity and Tissue Morphology. Cytotoxicity following exposure to 3R4F CS or THS2.2 aerosol was assessed by measuring the activity of AK released from the organotypic cultures into the basolateral medium. Figure 2 illustrates that

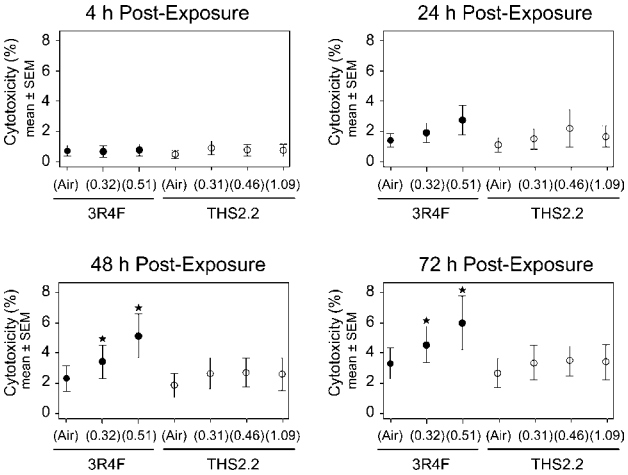


Figure 2. Cytotoxicity in organotypic cultures exposed to 3R4F CS or THS2.2 aerosol. Mean cytotoxicity levels were determined using the AK assay at various postexposure time points. The AK levels were normalized relative to those in the positive control (Triton-X-treated cultures considered to represent 100% cytotoxicity). Error bars indicate SEM (N = 11−13). Nicotine concentrations in 3R4F CS or THS2.2 aerosols are indicated for each group (mg/L, x-axis). * $p < 0.05$, compared with the corresponding air control.

3R4F CS-exposed cultures showed more cytotoxicity than air-exposed controls (48 and 72 h postexposure). However, the very low cytotoxicity (maximum approximately 6%) indicated that the organotypic cultures were highly resistant to CS impact at the selected CS concentrations, which is in line with our experimental design, aimed to cause moderate damage to the cell cultures. The THS2.2 aerosol-exposed cultures showed no cytotoxicity, as in the air-exposed controls, regardless of exposure, concentration, or time.

Oral organotypic cultures were embedded in paraffin at 48 and 72 h after exposure, sectioned and stained with H&E. No relevant morphological changes were observed at earlier postexposure time points (data not shown). Representative H&E sections from the 4 experimental repetitions are shown in Figure 3. The EpiOral tissue model used in this study consists of normal human oral epithelial cells organized in a basal layer and multiple noncornified layers (in total, approximately 20−30 layers), analogous to the structure of native human buccal epithelial tissue.

The images show similar tissue morphologies at the 48 and 72 h postexposure time points in air-exposed controls. At 48 h postexposure, the morphology of cultures exposed to 3R4F CS was similar to that of the air control. However, some cellular detachment above the basal cell layer was detectable in cultures exposed to 3R4F CS at both doses (0.32 and 0.51).

DOI: 10.1021/acs.chemrestox.6b00174
Chem. Res. Toxicol. 2016, 29, 1252−1269

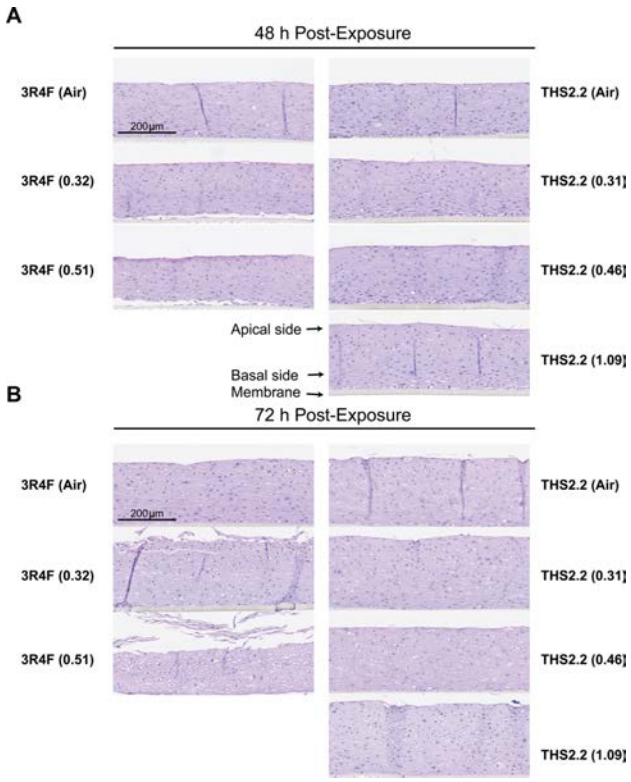


Figure 3. Tissue morphology after 3R4F CS or THS2.2 aerosol exposure. Representative images of H&E stained oral culture sections observed at 48 (A) and 72 (B) h postexposure. Staining was performed as described in Materials and Methods. The applied nicotine concentration (mg/L) for each condition is shown in parentheses; 20× magnification. $N = 12$.

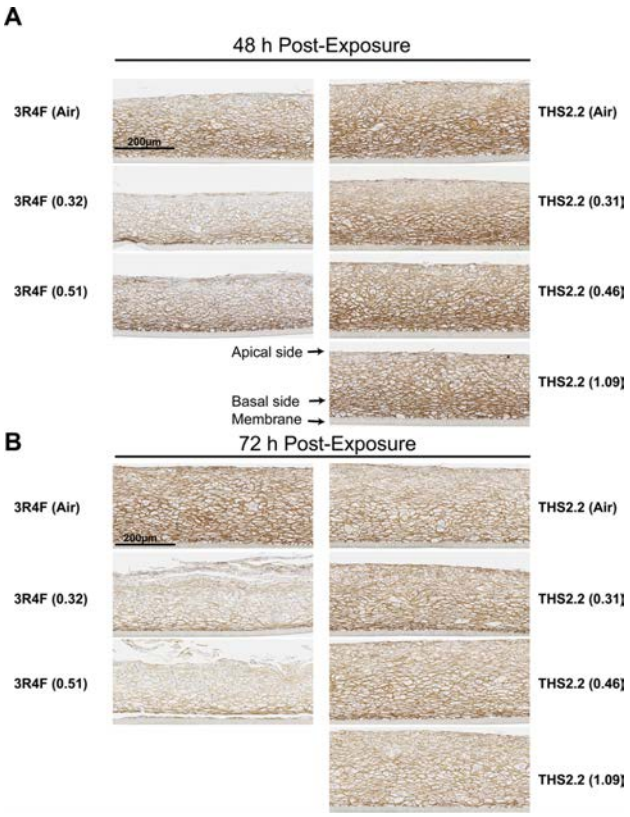


Figure 4. E-cadherin stained organotypic oral cultures after 3R4F CS or THS2.2 aerosol exposure. Representative images of E-cadherin stained oral culture sections observed at 48 (A) and 72 (B) h postexposure. Staining was performed as described in Materials and Methods. The applied nicotine concentration (mg/L) for each condition is shown in parentheses; 20× magnification. $N = 12$.

At 72 h postexposure to 3R4F CS, cultures exhibited signs of damage, with detachment above the basal cell level, as well as signs of adaptation, e.g., apical keratinization, desquamation, and intracellular granular structures. These effects were more prominent with the higher 3R4F CS concentration (0.51). In contrast, organotypic cultures exposed to the THS2.2 aerosol showed no relevant signs of toxicity at any of the concentration tested, except for a light desquamation with exposure to the higher doses (0.46 and 1.09). For scoring related to each morphological finding, see Figure S4.

A DRA phase was performed once the experimental repetitions were completed to investigate cellular responses to additional concentrations of THS2.2 aerosol. We exposed organotypic cultures to the following aerosol concentrations (nicotine concentrations in mg/L indicated in parentheses): 25% (0.34), 32% (0.45), 80% (1.02), and 100% (undiluted, 1.79) (Figure S5) and measured cytotoxicity and tissue morphology at 72 h post-exposure, the time point at which greatest alterations were observed in the other experiments (Figure 3). Three independent exposure runs were performed for this concentration range assessment. Neither tissue damage (Figure S5A) nor cytotoxicity (Figure S5B) was observed at 72 h postexposure at any of the THS2.2 concentrations tested. This indicates that even the fully concentrated THS2.2 aerosol had no apparent toxic effects on oral organotypic cultures when administered as an acute exposure.

We stained oral organotypic cultures for E-cadherin. E-Cadherin is a calcium-dependent adhesion molecule[56] and acts as an adhesion receptor in the adherens junctions, with important functions in cell−cell adhesion and cell signaling.[56,57] Control tissues had marked basal and supra-basal staining outlining the cells, whereas 3R4F CS-exposed tissues showed decreased staining, even 48 h after exposure (Figure 4A). At 72 h postexposure, staining for E-cadherin was decreased even further (Figure 4B). Overall, the exposure to THS2.2 aerosol did not alter the level of E-cadherin staining at both postexposure time points (Figure 4) with the exception of a slightly reduced immunostaining that can be observed only for the highest THS2.2 aerosol concentration (1.09) after 72 h postexposure (Figure 4B), although not comparable to the intensity observed for 3R4F CS-exposed cultures.

Alterations of CYP1A1/CYP1B1 Activity. Primarily aimed at detoxification and elimination of xenobiotics (phase I metabolism), cytochrome CYP450 enzymes metabolize several toxicants present in CS, such as polycyclic aromatic hydrocarbons (PAHs), nitrosamines, acrylamines, and nicotine. However, some of the metabolites generated are highly reactive genotoxicants and carcinogens. Both CYP1A1 and 1B1 are inducible in the lung by smoking and play key roles in metabolism of PAHs.[58] They can also be induced in the buccal epithelium *in vivo* and *in vitro*.[59]

The combined activity of CYP1A1 and CYP1B1 enzymes was measured in organotypic oral cultures at 24 and 48 h following exposure. Figure 5 shows that although at 24 h postexposure a dose-dependent decrease could be inferred, there were no significant changes in CYP activity in 3R4F CS-exposed cultures, compared with air-exposed controls. In contrast, a dose-dependent increase in CYP1A1/CYP1B1 activity, up to 15%, was observed in cultures exposed to THS2.2 aerosol at both

DOI: 10.1021/acs.chemrestox.6b00174
Chem. Res. Toxicol. 2016, 29, 1252−1269

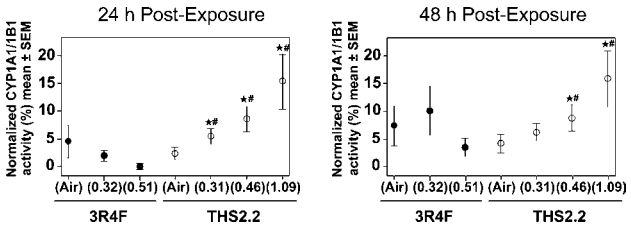


Figure 5. Alteration of CYP1A1/CYP1B1 activity following 3R4F CS or THS2.2 aerosol exposure. The combined activity levels of CYP1A1/CYP1B1 were normalized relative to those in the positive control (TCDD-treated cultures considered as having 100% activity). Error bars indicate SEM ($N = 12$). Nicotine concentrations in the smoke or aerosol are indicated for each group (mg/L, x-axis). * $p < 0.05$, compared with the corresponding air control. # $p < 0.05$, compared with matching concentrations of 3R4F CS or for THS2.2 (1.09), with 3R4F (0.51).

postexposure time points. In addition, CYP activity was significantly higher in cultures exposed to THS2.2 than in those receiving comparable concentrations of 3R4F CS, when measured at 24 h. At 48 h postexposure, this was the case with only one concentration of THS2.2 (0.46). An AK release cytotoxicity assay was performed, as a control, to test the basolateral medium of the same culture inserts also used to measure CYP activity. The results indicated no cytotoxicity due to the addition of CYP substrate for the measurements and were consistent with those illustrated in Figure 2 (data not shown).

Profiles of Secreted Proinflammatory Mediators. To assess the impact of 3R4F CS or THS2.2 aerosol on the production of proinflammatory mediators, we measured concentrations of cytokines, chemokines, and growth factors in the basolateral medium of EpiOral cultures at different times after exposure (24, 48, or 72 h). Four hour postexposure analyses were not considered for this end point: the secretion of the cytokines in basolateral media increased with increasing postexposure time (based on previous observation; data not shown); therefore, at 4 h postexposure there was a higher chance of having measurements below the detection limits.

In general, at all time points, cultures exposed to 3R4F CS had altered levels of secreted proinflammatory mediators, when compared with their respective air-exposed controls. In particular, VEGFA, TGFA, MMP-1, and IL1β concentration in the medium was significantly increased after 3R4F CS exposure (Figure 6). THS2.2 aerosol, at comparable nicotine concentrations, was also linked to increased levels of these mediators significantly, though to a lesser degree and at fewer time points, as compared with 3R4F CS exposure. In contrast, CSF3 levels were significantly higher after THS2.2 aerosol but not after 3R4F CS exposure, mainly at the 48 h time point. Some mediators were downregulated after 3R4F CS exposure, in particular CXCL8, CXCL10, IL6, and CSF2. Of these, CXCL10 was also downregulated after THS2.2 aerosol exposure.

Exposure to the highest THS2.2 aerosol concentration (1.09 mg/L) led to slight alterations in levels of all inflammatory mediators when compared with the lower THS2.2 aerosol concentrations (0.31 and 0.46 mg/L). However, the fold-changes were lower than those observed in CS-exposed cultures. Individual bar graphs for each analyte are presented in Figure S6.

Exposure Impact on mRNA Profiles. As reported in the previous sections, cytotoxicity and tissue damage were moderate in organotypic cultures exposed to 3R4F CS and very limited or absent in those exposed to THS2.2 aerosol. The absence of gross damage and cell death made it possible to safely investigate toxicity-specific mechanisms associated with exposure at all of the concentrations of 3R4F CS and THS2.2 aerosol tested. To do this, we generated gene expression data using standard Affymetrix array-based technologies and a standard and reproducible bioinformatics pipeline based on updated open-source software (see Materials and Methods). In the next paragraphs, we describe our results on mechanistic networks and gene pathways and focus on relevant individual marker genes.

Mechanistic Networks and Gene Pathways. The hierarchical organization of the collection of networks used in our systems toxicology approach enabled us to assess the biological impact of each exposure, 3R4F CS or THS2.2 aerosol, first at a high level of mechanistic description, as defined by the four network families (Figure 7, panel BIF).[60] The collection of networks covers a wide range of biological processes in the pulmonary system, which were a priori considered as relevant to capture the response of 3R4F CS-exposed oral epithelial tissue models (Table 2).[23] Relative to air-exposed controls, a higher

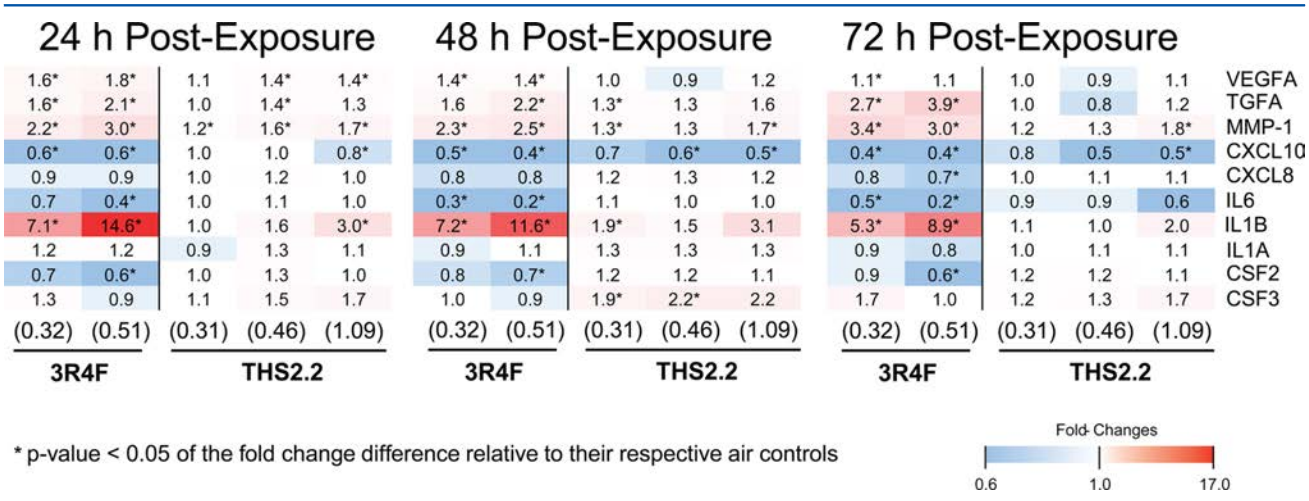


Figure 6. Profiles of secreted proinflammatory mediators following exposures. Heatmap showing the fold-changes of the mean concentrations of proinflammatory mediators in exposed cultures relative to those in their corresponding air controls at 24, 48, or 72 h postexposure for each group. Blue and red indicate negative or positive fold-changes, respectively, in the 3R4F CS- and THS2.2 aerosol-exposed, as compared with air-exposed, samples. Nicotine concentrations in the smoke or aerosol are indicated for each group (mg/L, x-axis). $N = 12$.

DOI: 10.1021/acs.chemrestox.6b00174
Chem. Res. Toxicol. 2016, 29, 1252−1269

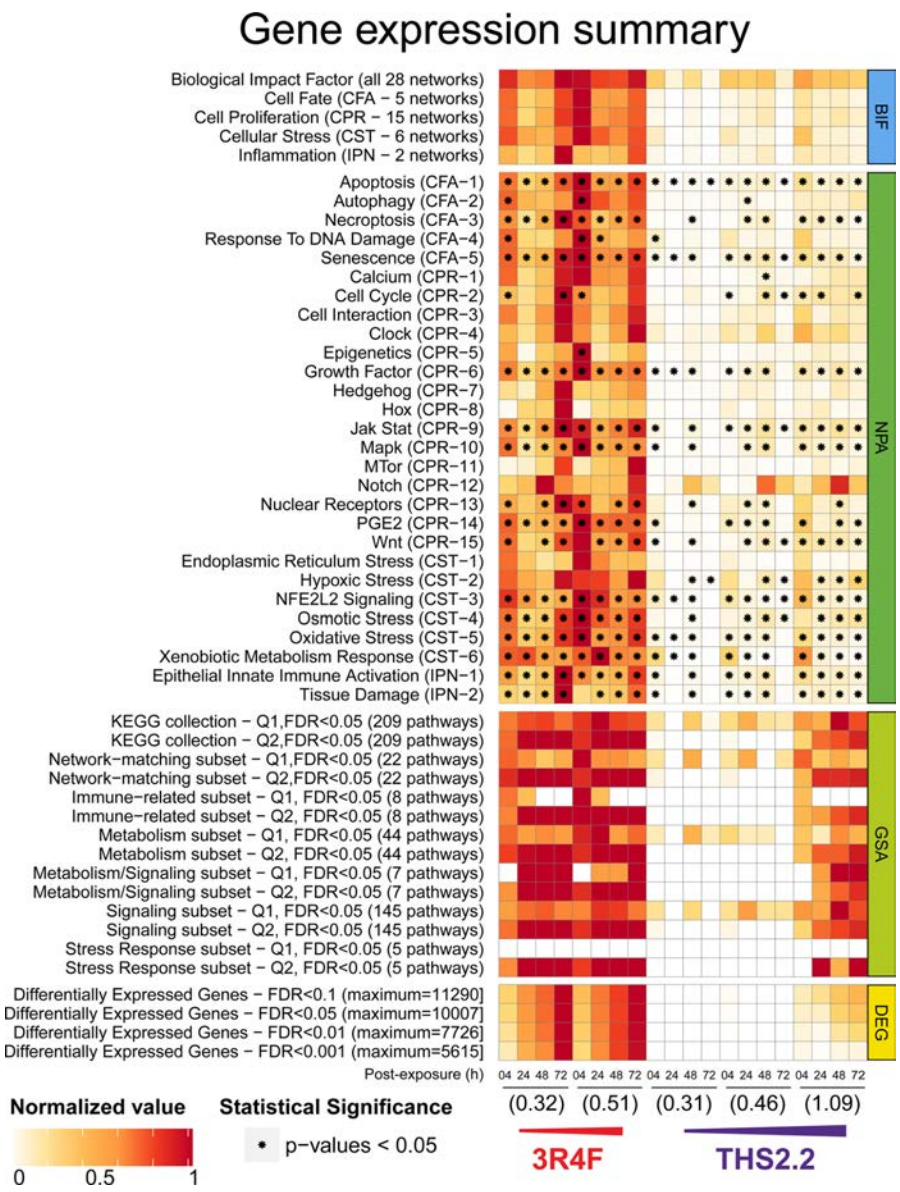


Figure 7. Overview of the impact of 3R4F CS or THS2.2 aerosol exposures on differential expression of genes. The values are normalized to the interval [0, 1] in a row-wise manner, and the details of their calculations and meanings are given in the Materials and Methods section. The uppermost panel displays the biological impact factor (BIF), which quantifies the overall impact of the exposures using the full suite of networks. It also includes the contribution of the four network family to the overall BIF (cell fate and angiogenesis−CFA, cell proliferation−CPR, cellular stress−CST, and pulmonary inflammation−IPN). The contributions of network families result from the aggregation of the perturbation amplitudes (NPAs) for each single network; these are shown for each relevant network in the middle panel. The "*" indicate statistical significance of the network perturbation, as explained in the Materials and Methods section. Overall results of gene set analyses (GSA) are displayed in the next panel as the counts of statistically significant gene sets for the KEGG collection and the two statistics (Q1 and Q2). Also shown are specific subsets of the KEGG collection: first the 22 pathways matching the mechanistic networks and second the 5 broad categories of the 228 pathways contained in the KEGG collection. Finally, the lowermost panel shows the number of differentially expressed genes (DEGs) for three distinct statistical significance thresholds, in order to identify possible threshold effects.

impact in all 3R4F CS-exposed cultures was detected, both at the global level (all 28 networks) and at the level of the four network families, with the two CS concentrations producing comparable effects. In particular, we observed a greater impact at 4 h postexposure for the CFA, CPR, and CST network families. This was decreased at 24 and 48 h postexposure, and then the impact of the exposure rose again at 72 h. In the THS2.2 aerosol-exposed cultures, we observed a significantly lower response at all concentrations tested, with no apparent trends.

In the NPA panel of Figure 7, the effects of 3R4F CS and THS2.2 aerosol exposures at the level of 28 network models are illustrated. Major significant perturbations on the network models were observed after 3R4F CS exposure in the subnetworks describing the biology of senescence, necroptosis, apoptosis (CFA), xenobiotic metabolism response, oxidative stress, osmotic stress, NFE2L2 signaling (CST), tissue damage, and epithelial innate immune activation (IPN). Exposure to THS2.2 aerosol minimally impacted these subnetworks, with only a small peak increase at 48 h for the CPR/Notch subnetwork.

We investigated whether the results obtained from our network-based systems toxicology approach were confirmed using the GSA approach. The GSA approach provides a less specific biological

DOI: 10.1021/acs.chemrestox.6b00174
Chem. Res. Toxicol. 2016, 29, 1252−1269

interpretation and is therefore more suitable for explorative research, whereas our systems toxicology approach has been specifically developed for the comparative assessment of exposure effects.[61] The first subset of KEGG pathways was selected to be analogous to the network models based on similarities among the key molecules described in the network models and the biology described in the KEGG pathways. The other five subsets were obtained by grouping the pathways by gene content and biological processes (see Materials and Methods). We applied two standard GSA statistical test procedures, Q1 and Q2, to assess the relevance of the corresponding biology (see Materials and Methods). The GSA panel of Figure 7 shows that most of the KEGG pathways matching our network models were significantly enriched after 3R4F CS exposure at all of the concentrations and time points. In contrast, THS2.2 aerosol exposure resulted in limited enrichment significances, mostly for the highest concentration (1.09 mg/L nicotine). These results were consistent with those obtained with the network-based approach. A detailed heatmap for the 22 network-matching pathways of the KEGG collection is shown in Figure S7.

The other GSA results displayed in Figure 7 and Figures S8 show similar trends, with Q1 statistical significance diminishing upon postexposure time. This is explained by the high number of large fold-change genes (see below) and clearly indicates that the choice of the enrichment statistics is crucial in order to correctly assess the biological impact of exposure.

The DEG panel (Figure 7) shows that the gene-level impact of 3R4F CS exposure on gene expression was greater than that of THS2.2 aerosol, causing a sustained response in time and amplitude which was not observed at any of the THS2.2 aerosol concentrations. At the highest concentration (1.09 mg/L), THS2.2 aerosol altered global gene expression with a proportional time-dependence, but by a much lower magnitude, compared with all 3R4F CS concentrations. An alternative representation of the gene expression profile without a statistical significance threshold is presented as volcano plots in Figure S9. Volcano plots represent the exposure-induced differential expression of all the measured genes (horizontal axis) against their statistical significance (vertical axis). They provide a useful depiction of the molecular-level effects of the applied exposure treatments.

Exposure Impact on Specific Marker Genes. We analyzed in more detail the expression of the genes contributing to perturbations in some of the subnetworks altered by 3R4F CS exposure. The heatmap in Figure 8 shows a selection of genes most impacted by 3R4F CS exposure. Increased expression of many of the genes regulating oxidative stress was observed in 3R4F CS-exposed cultures at all time points. These included *SLC7A11*, *HMOX1*, *GCLM*, *GCLC*, *TXNRD1*, *NQO1*, *GPX2*, and *NFE2L2*. Other oxidative stress-related genes showed decreased expression in the samples, including *MT1X*, *SLC40A1*, *XDH*, *CAT*, *GSTA4*, *SOD1*, *ID3*, and *MAF*. At all time points, expression levels of genes involved in xenobiotic metabolism, such as *CYP1A1*, *CYP1B1*, and different *AKR* (*1C1/1C2/1C3*) in 3R4F CS exposed cultures were even higher.

3R4F CS exposure also substantially altered the expression levels of genes important for the inflammatory response in the cultures, like *MMP1*, *MMP10*, *IL1A*, *IL1B*, *IL1R2*, *CTGF*, *PTGS2*, and *CXCL14* (Figure 8).

In contrast, at comparable nicotine concentrations, THS2.2 aerosol exposure had a minimal (mainly limited to the 4 h postexposure) or no effect on the expression of most of these genes.

Expression levels of more genes were altered after exposure to the highest nicotine concentration of THS2.2 aerosol (1.09), though these fold-changes were lower than those observed in 3R4F CS-exposed cultures (for a more detailed list of genes see Figure S10).

In addition, Figure 8 shows the heatmap of genes reported as markers of normal buccal epithelial differentiation or previously described in non-neoplastic lesions and in reconstituted *in vitro* tissues.[25,62−68] Exposure to 3R4F CS resulted in decreased expression of the majority of cytokeratins (*KRT*) constituting the cytoskeletal intermediate filaments. In these samples, mRNAs for only *KRT7*, *KRT16*, and *KRT19* increased sporadically at a few time points, while *KRT17* was consistently upregulated at 24, 48, and 72 h. The RNAs of the keratinization-related genes involucrin (*IVL*) and filaggrin (*FLG*) increased with postexposure duration, and higher levels of the neuroendocrine markers *S100A1* and chromogranin A (*CHGA*) were sporadically observed.

Initial decreases at 24 h followed by late (72 h) increases in mRNA were observed for integrin, *ITGA6*, and, with similar kinetics, the protease, *KLK7* (Figure 8). A sustained increase in *MAPK14* expression was seen at all time points, except for 4 h of postexposure, with no obvious time- or concentration dependence. Expression of *MKI67*, a marker for cells active in the cell cycle, was increased only at the late time points, also without concentration dependence, while that of the proliferating cell nuclear antigen (*PCNA*) was lower at the later time points. Expression of the antimicrobial peptide, beta defensin-1 (*DEFB1*) was consistently increased with an early onset at 4 h, a transient maximum level from 24 to 48 h, and a decline at 72 h; moreover, this response was more pronounced with the higher concentration of 3R4F CS.

Exposure to the THS2.2 aerosol did not cause any significant mRNA changes at the low and medium concentrations (0.31 and 0.46) (Figure 8). The high THS2.2 concentration (1.09) elicited some changes reminiscent of the 3R4F CS-induced changes but of lesser magnitude. In these samples, expression of *KRT1*, *KRT2*, *KRT16*, *KRT76*, *KRT5*, and *KRT10* was also decreased, and there were, sporadically observed, slight increases in expression of *KRT15*, *KRT17*, and *KRT19*. Likewise, expression of *IVL* (but not *FLG*) and *ITGA6* was slightly higher than that in the controls at the later time points.

Because a loss of the adhesion molecule E-cadherin was observed in histological sections, we investigated the expression of genes involved in cellular adhesion. The heatmap in Figure 8 shows that 3R4F CS exposure caused a time- and dose-dependent downregulation of expression of the E-cadherin gene, *CDH1*. Other *CDH* genes (*CDH2*, *3*, *4*, and *5*) were not strongly impacted, with only small increases in expression at the latest time points. Desmosomes are intercellular junctions that contain two specific cadherins, desmocollin (*DSC*) and desmoglein (*DSG*). Expression of these cadherins is crucial for the correct assembly of the desmosome and, therefore, for cell−cell adhesion.[69] Interestingly, in our data set, we observed that genes encoding for these proteins (*DSG1*, *2*, and *3* and *DSC1*, *2*, and *3*) were substantially downregulated by exposure to 3R4F CS but not THS2.2 aerosol, at comparable nicotine concentrations. *PVRL* genes encode for nectins, a family of proteins involved in calcium-independent cellular adhesion.[70] Nectins are involved in various cell−cell junctions, in cooperation with or independently of cadherins.[71] We found that different *PVRL* genes responded differently to 3R4F CS. While *PVRL2* was substantially upregulated, *PVRL4* was significantly downregulated. Again, no gene expression alterations were observed after THS2.2 aerosol exposure. The Notch signaling pathway was described as regulating keratinocyte adhesion.[72] We found that expression of

DOI: 10.1021/acs.chemrestox.6b00174
Chem. Res. Toxicol. 2016, 29, 1252−1269

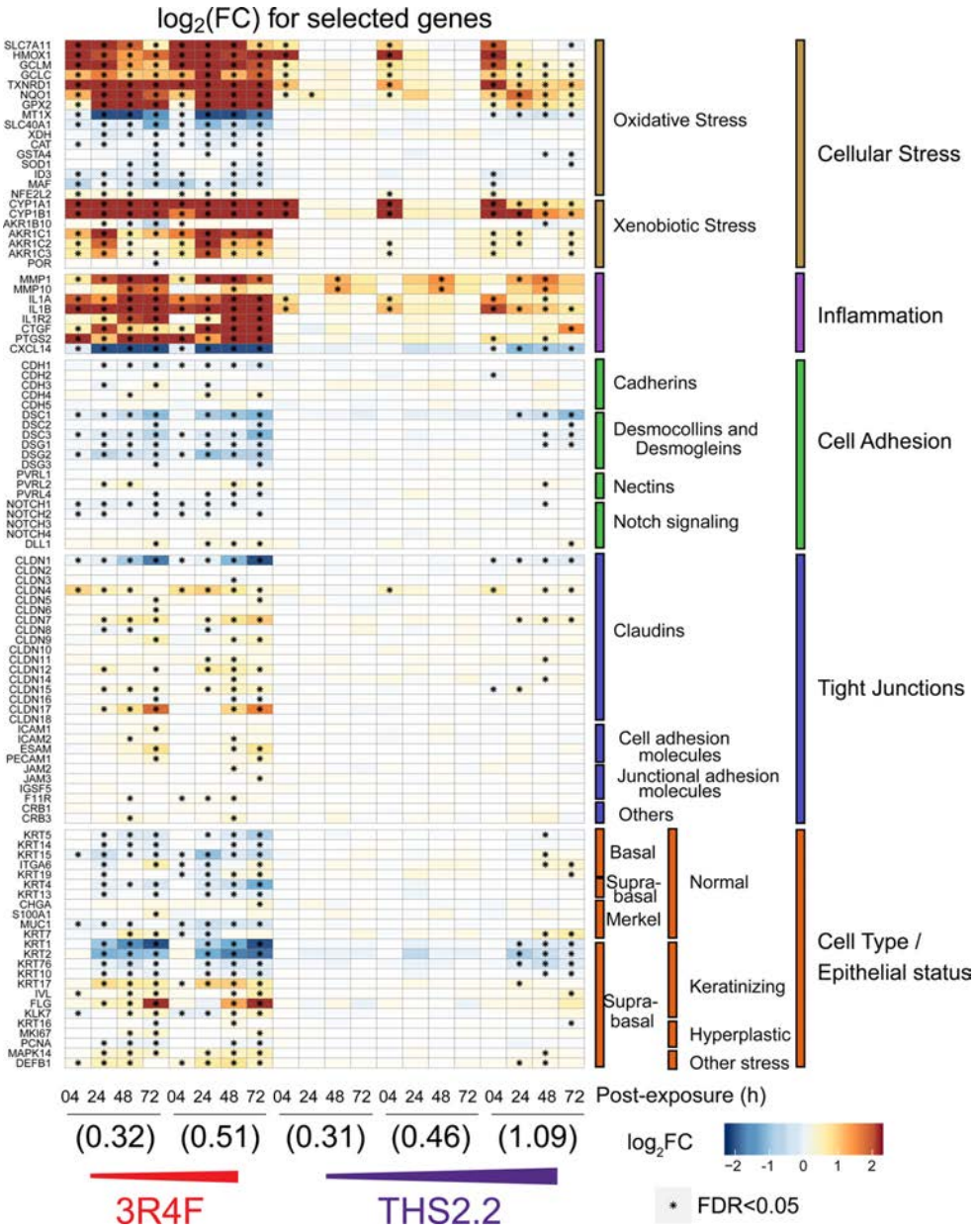


Figure 8. Impact of 3R4F CS and THS2.2 exposures on selected genes from different networks. The heatmap shows changes in gene expression expressed as $\log_2$(fold-change). Expression levels of up- and downregulated genes are compared with those in the corresponding air controls. Gene symbols are listed on the left of the heatmap. Stress-related processes are marked on the right of the heatmap. The "*" indicates statistically significant gene differential expressions based on FDR values smaller than the 0.05 threshold, as explained in the Materials and Methods section.

NOTCH1 and *NOTCH2* was strongly decreased by 3R4F CS exposure. Conversely, that of *DLL1* was increased. No effects on these genes were observed after THS2.2 aerosol exposure.

Claudins are pivotal barrier components of the tight junctions (TJ) and are involved in membrane permeability control.[73,74] Levels of several claudin mRNAs, in particular *CLDN4*, *CLDN7*, and *CLDN17*, were significantly increased with 3R4F CS exposure. Among the claudin genes analyzed, only *CLDN1* was downregulated. THS2.2 aerosol caused sporadic alterations in this subset of genes, primarily at the highest concentration (1.09 mg nicotine/L). Other genes involved in TJ formation, including *ICAM1/2*, *PECAM1*, *ESAM*, *JAM2/3*, *F11R*, and *CRB3*, also showed increased expression after 3R4F CS but not THS2.2 aerosol exposure. For a more comprehensive list of genes, see Figure S10.

Exposure Impact on miRNA Profiles. As post-transcriptional regulators, miRNAs influence many biological processes.[75] Possible mechanisms associated with the responses to 3R4F CS and THS2.2 aerosol exposures may be further inferred from the miRNA transcriptomics data. We obtained these data from oral organotypic cultures exposed to 3R4F (0.32), 3R4F (0.51). THS2.2 (0.31), THS2.2 (0.46), and THS2.2 (1.09), at all post-exposure time points.

The number of miRNAs whose levels were altered upon exposure to 3R4F CS increased with concentration and with post-exposure time (Figure 9 and Figure S11). At comparable nicotine concentrations to 3R4F CS, THS2.2 aerosol exposure was not linked to any effects on miRNA. We observed only one miRNA upregulated (miR-375) and one downregulated (miR-4521) by

DOI: 10.1021/acs.chemrestox.6b00174
Chem. Res. Toxicol. 2016, 29, 1252−1269

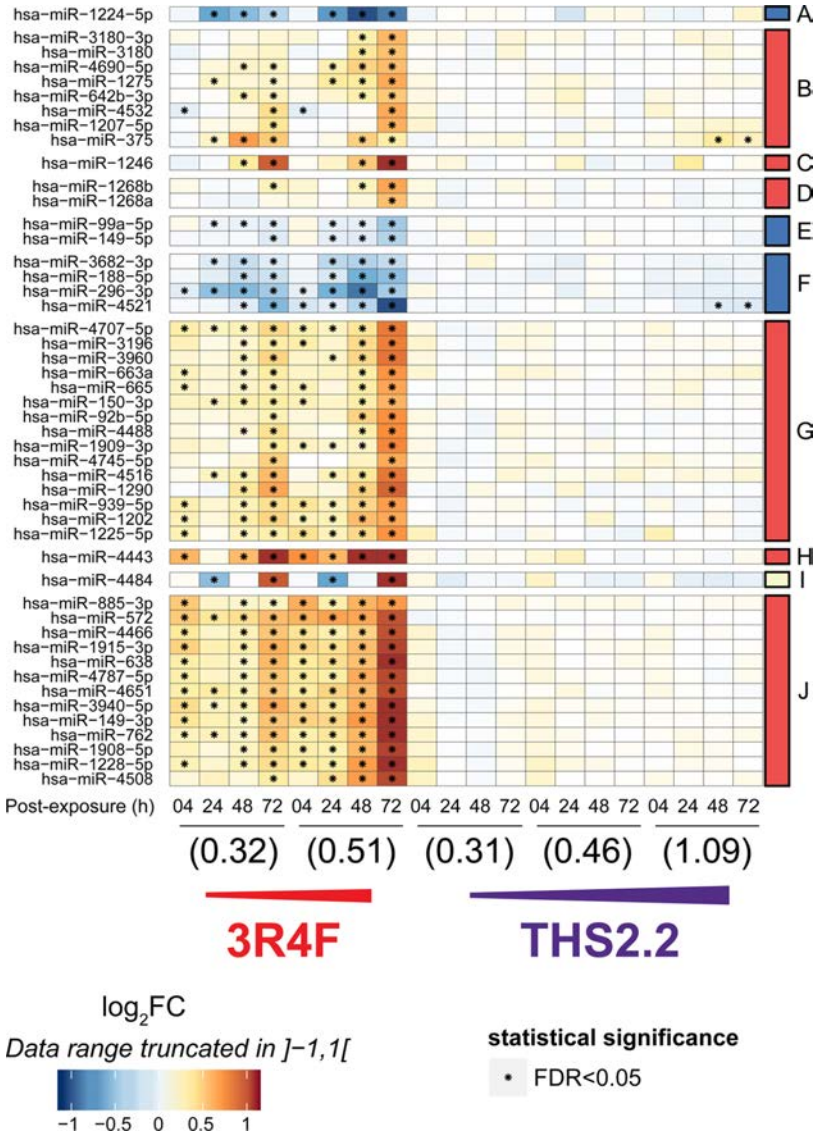


Figure 9. Exposure impacts on global miRNA expression. The heatmap shows the miRNAs that were significantly altered, with fold-changes of at least 0.5 (*) in at least one contrast (exposed group vs air control). The color gradient represents alteration of the miRNA levels ($\log_2$(fold-change)). For details, see Materials and Methods.

THS2.2 aerosol exposure, and this was only observed at the highest nicotine concentration. Regarding the biological functions of the responding miRNAs, we calculated the KEGG pathway enrichments of their anticorrelated potential gene targets (Table S3). Although the enriching genes represented only a small fraction of the anticorrelated targets, we observed several meaningful biological processes associated with them, which agreed with those obtained using the network-based approach.

Correlation of the Outcomes Across the Experimental Repetitions. Within the aims of this study, a comparative assessment of exposure effects of THS2.2 aerosol versus CS from 3R4F, it was important to demonstrate the robustness of the *in vitro* oral culture systems and our study design in combination with the applied statistical and computational approaches. We investigated the potential variability introduced by conducting the study over various experimental repetitions and found it to be minimal. To investigate the variability among experimental repetitions, separately for each end point, treatment, and post-exposure duration, the average of the differences between exposed and nonexposed measurements was computed for experiments 1 and 2 and compared with the average computed for experiments 3 and 4. These values are presented in Figure S12. The Spearman correlation coefficient indicated good reproducibility among the various experimental repetitions.

Reproducibility of mRNA or miRNA expression data revealed that, at the different postexposure time points, the gene expression changes in tissues exposed to 3R4F (0.32) and 3R4F (0.51) were highly correlated between those obtained in experiments 1 and 2 and those obtained in experiments 3 and 4 (Figure S13). Nonetheless, correlations were lower between gene expression fold-changes in THS2.2 aerosol-exposed tissues. This was expected because only a small number of genes were differentially expressed following THS2.2 exposure, as compared with CS exposure.

DISCUSSION

Our findings address the impact of conventional 3R4F CS and an aerosol from the candidate MRTP, THS2.2, on oral organotypic

DOI: 10.1021/acs.chemrestox.6b00174
Chem. Res. Toxicol. 2016, 29, 1252−1269

cultures. In line with the principle of the 3Rs[39] and the 21st Century Toxicology framework,[76−78] our study was designed to obtain robust and reproducible data, comparing the biological effects of CS and THS2.2 aerosol on human oral epithelium in a systems toxicology framework. We exposed the cultures for 28 min: we chose this time window based on the previously reported duration-dependent response of MMP-1 secretion; the secretion of MMP-1 was considered as a control for the responsiveness of organotypic airway cultures to CS.[79] Mathis et al. reported that the highest concentration of secreted MMP-1 was observed in a 3-D bronchial culture model after 28 min of exposure to 3R4F CS, as compared with 7, 14, and 21 min of 3R4F CS exposure.[79]

We leveraged *in vitro* cellular assays, combined with network-based computational modeling, to identify cellular and molecular alterations caused by these exposures. However, our current approach for using organotypic cultures has some limitations: (1) they were derived from a single donor, indicating that reproducibility of the system must be confirmed in the future by comparing results obtained in cultures derived from different donors; (2) only acute exposure effects were investigated, though a repeated exposure study might better elucidate long-term effects of CS and THS2.2 aerosol exposures. A chronic study would require validation of the stability of differentiation in these organotypic cultures over a prolonged period, in the presence and absence of fibroblasts, which normally contribute to the endurance of epithelial cells.[80] So far, chronic investigations have been addressed in only one publication: Chinnathambi et al. observed stable organotypic differentiation during 4 to 8 weeks of culture at the ALI in fibroblast-containing reconstructed human oral mucosa.[81]

Prior to our experiments, we selected 3R4F cigarette smoke and THS2.2 aerosol concentrations based on DRF results (data not shown for THS2.2). The criterion for selection was that the concentrations would elicit limited cellular damage, to enable us to infer toxicity-related mechanisms associated with exposure, instead of reflecting morphological alterations associated only with severely damaged tissue.[55] On the basis of the DRF phase, the organotypic cultures tolerated CS exposure, with little damage observed at up to 30% CS. Above 40 to 50% CS, considerable disintegration of their tissue-like structure occurred, while AK release was still moderate. In terms of morphological integrity, the higher CS concentration was, therefore, close to the MTD. For THS2.2 exposure, aerosol concentrations as high as 80% did not affect morphological integrity.

Our measurements showed that the selected nicotine concentrations were stable over experimental repetitions and that the applied dilutions correctly yielded the predicted matching concentrations of 3R4F CS and THS2.2 aerosol.

The characterization of 3R4F CS and THS2.2 aerosol also included measurement of various deposited carbonyls for each applied dilution. We observed that, at comparable nicotine concentrations, the levels of representative carbonyls were always higher in 3R4F CS than in THS2.2 aerosols.

Gross tissue damage in response to CS or aerosol exposure was assessed by measuring cytotoxicity using the AK release assay and by histology. The AK assay results showed that overall cytotoxicity was not high (approximately 6% maximum AK release in 3R4F CS-exposed samples) but was slightly higher in cultures exposed to 3R4F CS, compared with that of THS2.2. These results were similar to those in our previous study.[23] Likewise, the current results confirmed our previous observation that the combined activities of CYP1A1 and CYP1B1 were not increased by 3R4F CS, despite their strong transcriptional upregulation. However, THS2.2 aerosol caused a concentration-proportional increase in CYP1A1/1B1 activity at 24 and 48 h postexposure. Other prototypic heat-not-burn products were reported to induce *CYP1A1* expression in rat lungs,[82] as did an aerosol of nicotine in PBS.[83] It is likely that constituents present in the 3R4F CS but not in THS2.2 aerosol elicited a tissue-specific response that may interfere with translation or post-translational processing of the CYP1A1/1B1 polypeptides, increasing their degradation or inhibiting their activities. Similar observations have been reported for alpha-tocopherol inhibited benzo[*a*]pyrene-induced CYP1A1 activity, likely as post-translational inhibition, in rat liver microsomes.[84] Moreover, metal-induced heme oxygenase potently inhibited TCDD-induced CYP1A1 enzyme activity in human and rat hepatocytes.[85−87] Notably, heme oxygenase (*HMOX1*) transcription was also strongly induced by 3R4F CS exposure at all time points but was only transiently increased (at 4 h) by the THS2.2 aerosol. In intestinal and hepatic cells and in cell-free microsomal systems, it has been demonstrated that reduced mRNA and protein levels of cytochrome P450 (CYP) oxidoreductase (POR) (an important electron donor for all CYPs) can significantly lower CYP activities including CYP1A1.[88−93] In the 3R4F CS-exposed organotypic oral epithelial cultures, there was no consistent downregulation of POR expression, only a weak decrease for the lower concentration at the 72-h time point (Figure 8), that could explain the post-transcriptional inhibition of CYP1A1/1B1 activity. However, it has been shown that heme oxygenase activity also depends on functional POR[94,95] and that in bacterial membrane expression systems, two different CYPs compete for the available POR.[96] Hence, one might speculate that also the induced heme oxygenase 1 would compete with the CYPs 1A1/1B1 for POR as the necessary electron donor; however, solid experimental evidence would be required to support such a mechanism. Other prototypic heat-not-burn products were reported to induce *CYP1A1* expression in rat lungs,[82] as did an aerosol of nicotine in PBS.[83]

We previously reported[23] that altered concentrations of proinflammatory mediators were secreted in the basolateral medium of organotypic cultures following 3R4F CS exposure.[23] Similar CS exposure effects were also observed in the present study, including increased secretion of IL1β, MMP1, VEGFA, and TGFA and decreased secretion of CXCL10, CXCL8, CSF2, and IL-6, compared with their levels in air-exposed controls. Overall, exposure to THS2.2 aerosol at comparable and even higher nicotine concentrations led to fewer and lower magnitude changes in the secretion of proinflammatory mediators, with the exception of CSF3, than did exposure to 3R4F CS.

In agreement with these findings, the network based approach revealed that the pulmonary inflammatory processes network was impacted by exposure to either CS or THS2.2 aerosol. Moreover, the lower fold-changes in the release of inflammatory mediators observed in THS2.2 exposed cultures were accompanied by a lower NPA score in the heatmap. In most but not all cases, there was a good correlation between changes in expression and secretion levels. Surprisingly, *IL1A* mRNA levels, which were significantly increased by 3R4F CS, did not correlate with the levels of secreted IL1α. We also found a lack of correlation of mRNA levels and abundance of secreted mediators in our previous study. Possible reasons include differences in the individual culture preparations that were used to measure the different end points (i.e., data were not longitudinal), a lack of translation to proteins, a lack of proteolytic processing, e.g., of the

DOI: 10.1021/acs.chemrestox.6b00174
Chem. Res. Toxicol. 2016, 29, 1252−1269

31 kDa precursor of IL1α by calpain,[97] a lack of secretion, or negative feedback of the accumulated cytokines on their own transcription.[23,98] In contrast to our previous findings, levels of IL6 were lower than those in the controls, which might be caused by the use of cultures with only epithelial cells for the present study. These cultures did not have the fibroblast monolayer underneath the epithelium, mimicking the lamina propria, as did the "full thickness" oral epithelial tissue model used in our previous study. Indeed, the secretion of mediators can be influenced by fibroblasts, as we recently demonstrated in a cocultured organotypic bronchial model.[80]

The buccal mucosa consists of a fibroblast- and collagen-rich lamina propria covered by a stratified, noncornifying, or keratinizing epithelium. Its structure and composition resemble, for example, the esophageal epithelium and differ from other regional types of oral epithelium, such as the keratinizing epithelia of the hard palate or the gingiva. Upon chemical or mechanical stress, injury, or inflammatory stimuli, the buccal epithelium can respond with keratinization, rendering it structurally similar to the gingival epithelium.[1,4] Desquamation is another well-known response of the buccal mucosa to irritants.[99] After 3R4F CS exposure, we observed increased ectopic/apical keratinization and desquamation. This finding was accompanied by an increased number of structures resembling granular material that are normally present in the stratum granulosum of keratinizing tissues. These observations might indicate the induction of differentiation processes toward the formation of cornified layers.[100−102] There is some resemblance to the weak adaptive response to repeated CS exposures, with minimal cytotoxicity and slightly increased tissue thickness and keratinization, that was reported to occur in buccal organotypic epithelial cells cocultured with fibroblasts.[23] In addition, keratinization was observed in healthy oral mucosa from smokers,[103] and Gualerzi et al. demonstrated that acute exposure of oral biopsies to CS led to a differentiation in the phenotype of keratinocytes, ultimately leading to supra-basal layer keratinization.[12]

No keratinization was observed in samples exposed to THS2.2 aerosol at any concentration tested. It was proposed that an increase in keratinized cells could be caused by volatile compounds in tobacco.[9,104] Hence, the presence of lower levels of aldehydes and other irritants could explain the reduced impact of THS2.2 aerosol on this histological feature. Only increased desquamation was found as a significant feature of THS2.2-exposed cultures. However, at comparable nicotine concentrations, THS2.2 exposed cultures had a lower score than did the 3R4F CS-exposed cultures.

3R4F CS induced other relevant histopathological modifications in the oral cultures, such as an enhanced incidence and severity of detachment above the basal cell level and longitudinal cleft formation. These were more prominent at 72 h post-exposure, regardless of the nicotine concentration, indicating a sustained response. Interestingly, detachment of the epithelium above the basal cell level was also observed in other 3D tissue types exposed to CS, like organotypic nasal and bronchial tissue cultures (data not shown). This finding could be related to impaired cell adherence. Indeed, we observed a consistent and diffuse decrease in E-cadherin staining in organotypic cultures exposed to 3R4F CS. This is in agreement with previous findings that E-cadherin and zonula occludens-1 were reduced after exposure of pretreated fibroblasts and immortalized keratinocytes to smokeless tobacco.[105] THS2.2 aerosol-exposed cultures, even at the highest nicotine concentration, showed no discernible alterations in these parameters when compared with those in air-exposed controls.

In support of the histological observations, no evident alterations in the transcriptional levels of a series of genes involved in keratinization, adhesion, and barrier formation were observed in THS2.2 aerosol-exposed organotypic cultures. For a detailed discussion, see Supporting Information, Discussion.

CONCLUSIONS

In this study, we investigated the effects of one acute exposure of buccal organotypic cultures to conventional CS or THS2.2 aerosol. The CS-induced histopathological modifications we observed in the organotypic cultures were supported by findings from our network-based approach. We demonstrated that the impact of the exposure (suggested by the NPA scores) was high and sustained over time. Similar to findings from a previous study on CS-exposed buccal epithelial cultures,[23] there was a significantly increased cellular stress network response primarily driven by the increased NPAs for xenobiotic metabolism, NFE2L2 signaling, and oxidative stress. In addition, several cell death- and senescence-related, inflammatory and cell cycle-related subnetworks were significantly perturbed. Such impacts were less clear in our previous study employing fibroblast-containing cultures.[23]

The observed gene expression changes induced by 3R4F CS exposure were consistent with features of *in vivo* epithelial adaptive responses to acute irritation. There were some, though incomplete, indications of induction of keratinization but no signs of tissue damage-induced regeneration (that is, no proliferative signaling or histological indications). Moreover, CS had apparently opposing effects on cell−cell contacts. We observed cellular detachment above the basal layer, likely related to the loss of adhesion proteins such as E-cadherin. In contrast, however, there was a moderate increase in mRNA expression of TJ components, indicating a reinforcement of the epithelial barrier in response to the irritating effects of smoke exposure.

Most importantly, this systems toxicology *in vitro* investigation on human organotypic buccal epithelial cultures, aligned with the 3Rs principles, demonstrated that acute exposure to THS2.2 aerosols did not cause gross toxicity or adaptive responses. Compared with CS exposure, THS2.2 aerosol exposure had an overall significantly lower impact on buccal epithelial physiology (except for a transiently higher CYP1A1/1B1 activity), as indicated by histopathological, inflammatory, and transcriptomics (both mRNA and miRNA) data. Furthermore, no novel effects of THS2.2 aerosol were detected.

ASSOCIATED CONTENT

Supporting Information

The Supporting Information is available free of charge on the ACS Publications website at DOI: 10.1021/acs.chemrestox.6b00174.

Supplementary Methods and Discussion sections and tables and figures (PDF)

AUTHOR INFORMATION

Corresponding Author

*Tel: +41 58 242 2214 Fax: +41 58 242 2811. E-mail: julia.hoeng@pmi.com.

Funding

This study was funded by Philip Morris Products S.A. (part of Philip Morris International group of companies).

DOI: 10.1021/acs.chemrestox.6b00174
Chem. Res. Toxicol. 2016, 29, 1252−1269

Notes

The authors declare the following competing financial interest(s): All authors are employees of, or (W. K. Schlage) contracted and paid by PMI R&D, Philip Morris Products S.A. (part of Philip Morris International group of companies). Philip Morris International is the sole source of funding and sponsor of this project.

Biographies

Dr. Filippo Zanetti has been a scientist at Philip Morris International R&D since 2015. He was trained in Biology at the University of Padua, Italy, where he also obtained his Ph.D. in biochemistry and biotechnologies. He continued his carrier as a postdoctoral researcher at the German Center for Neurodegenerative Diseases (DZNE) in Bonn and at the Centre Médical Universitaire (CMU), Geneva, Switzerland. His current work involves the assessment of the effects of tobacco smoke and modified risk tobacco products in oral human organotypic cell culture models.

Dr. Alain Sewer obtained his Ph.D. degree in physics at the University of Neuchâtel, Switzerland, with research focus on theoretical models for high-temperature superconductivity. Afterward, he occupied postdoctoral researcher positions in computational biology at the Universities of Basel and Lausanne and principally focused on the understanding of microRNA regulation of gene expression. At present, he is a scientist in data modeling at Philip Morris International R&D where he applies quantitative network-based systems toxicology approaches to the assessment of modified risk tobacco products.

Dr. Carole Mathis has been a scientist at Philip Morris International R&D since 2008. She obtained her Ph.D. in molecular and cellular biology at the University Louis Pasteur (Strasbourg, France). Subsequently, she worked as a postdoctoral researcher at the Rockefeller University, New York, USA, and at the University of Zurich, Switzerland. She is currently leading different projects on the assessments of tobacco smoke and modified risk tobacco products, utilizing (3D) air−liquid interface and (2D) primary cell culture models.

Dr. Anita R. Iskandar has been a scientist at Philip Morris International R&D since 2013. She was trained in biochemistry and molecular nutrition and completed her doctoral degree at Tufts University, Boston, MA, USA. Her previous work focuses on the nutritional aspect of lung cancer prevention. Her current work involves an assessment of the effects of tobacco smoke and modified risk tobacco products using three-dimensional organotypic human airway culture models.

Dr. Radina Kostadinova obtained her Ph.D. degree in biochemistry in 2005 at the University of Bern, Switzerland with focus on the study of the transcriptional control of kidney enzymes in inflammatory conditions. Afterward, she continued her career taking postdoctoral positions at University of Lausanne and Zurich, Switzerland to work on various disease areas such as liver fibrosis, inflammation, diabetes, and obesity. Her last two positions as a scientist were at Hoffmann-La-Roche and Philip Morris International R&D, Switzerland, with research focus to develop and establish 3D tissue models for detection of drug- or cigarette smoke-induced toxicity.

Dr. Walter K. Schlage is a free-lance scientific consultant in biology and toxicology since 2013. He was trained in cell and developmental biology, genetics, and biochemistry (Ph.D.) and gained special experience in inhalation toxicology, experimental carcinogenesis, *in vitro* technologies, and computational modeling during his affiliation with various Philip Morris International research organizations for over 25 years. Dr. Schlage is especially interested in multidisciplinary approaches, particularly systems toxicology, and the focus of his current collaboration with Philip Morris International R&D is on tobacco smoke-related disease models, modified risk tobacco products, and the synthesis of classical toxicology, molecular biology, and *in silico* modeling.

Dr. Patrice Leroy obtained his Ph.D. in applied mathematics at university of Saint-Etienne with research focus on tomographic imaging and detector design. Afterward, he joined EMPA at Dübendorf as a guest scientist and ISMECA at La-Chaux-de-Fond as a vision algorithm specialist. Since 2009, he has been a statistician for *in vivo*, *in vitro*, and clinical studies for companies such as Merck-Serono, Hoffmann-La Roche, and Philip Morris International R&D.

Shoaib Majeed was born in 1986 and received his Master's degree from Martin Luther University, Germany. He joined Philip Morris International R&D in April 2012. In his current role, he is responsible for the generation of aerosols from Modified Risk Tobacco Products and conventional cigarettes, and organizes and performs *in vitro* aerosol exposures of complex 3D organotypic cell cultures grown at the air−liquid-interface using *in vitro* exposure systems.

Emmanuel Guedj has been working as a supervisor of the Transcriptomics team at Philip Morris International R&D in Neuchâtel (Switzerland) for 4 years. He has been working in collaboration with the System Toxicology team to carry out gene expression analysis and identify gene signatures and biomarkers of exposure. Prior to joining Philip Morris International, he had a position in the Biomarker Discovery department at Merck-Serono in Geneva and was in charge of a gene expression platform at the University of Medicine of Marseille (France). His main focus is on gene expression profiling using GeneChips, miRNA in exosomes, and qPCR.

Keyur Trivedi is a UK-Health and Care Professions Council registered Biomedical Scientist and holds M.Phil. in Life Sciences and M.Sc. in Biomedical Technology from Gujarat University, India. He has held various positions in research, diagnostics, and healthcare sectors mainly focusing on the field of histopathology.

Dr. Florian Martin is Principal Mathematician at Philip Morris International R&D in Switzerland. Florian obtained his Ph.D. degree in theoretical mathematics in 2003 from the University of Neuchatel, Switzerland and holds two Master's degrees in mathematics and in statistics. Florian has 13 years of experience in the field of bioinformatics, computational biology and biostatistics. His current research focus in systems toxicology is on the development of novel network based approaches and computational methodologies to facilitate the understanding of the mechanisms of disease and toxicity.

Dr. Ashraf Elamin graduated from Duquesne University in Pittsburgh, PA, USA with a Ph.D. in biochemistry in 2005. Prior to joining Philip Morris International R&D in 2010, he worked as a Manager of the Proteomics Core Facility at California State University Long Beach from 2006 to 2010. Currently at Philip Morris International, he manages the Proteomics and Lipidomics team, which is responsible for performing quantitative proteomics and lipidomics analyses on biological samples for product assessment.

Céline Merg obtained her M.Sc. in molecular and cellular biology at the University Joseph Fourier in Grenoble, France. She worked previously at Novartis in the biomarker development department. She joined Philip Morris International R&D 4 years ago, and she is responsible for the antibody-based platform in the Proteomics team.

Dr. Ivanov Nikolai currently holds the position of Manager of the Research Technologies department at Philip Morris International R&D Innovation Cube, Philip Morris Products S.A. in Neuchatel, Switzerland. In this role, he is responsible for setting the strategic direction of the department and leading genome sequencing, gene expression, proteomics, high performance computing, and quality management systems projects. He received his M.Sc. in mathematics and computer

DOI: 10.1021/acs.chemrestox.6b00174
Chem. Res. Toxicol. 2016, 29, 1252−1269

science in 2001 and his Ph.D. in biochemistry in 2002 from Emory University (Atlanta, GA, USA). He has published more than 30 manuscripts primarily in the area of systems biology. In 2015, he was awarded the title of *Privat Docent* by the University of Neuchatel (Switzerland).

Dr. Stefan Frentzel, after his Ph.D. in molecular and cellular biology (University of Heidelberg, Germany) and postdoctoral research at Sandoz Pharma Ltd., became a Research Investigator at Novartis Institutes for BioMedical Research (Basel, Switzerland), working as a key team member and project team head in target identification and validation, development of biologics, and cell-based assays for drug profiling. He later accepted a position as Supervisor Antibody-based Proteomics at Philip Morris International (Neuchâtel, Switzerland) and shortly after got appointed to Manager Cellular Laboratories. In his current position, he manages laboratories for *in vitro* safety assessments of modified risk tobacco products, utilizing (3D) air−liquid interface and (2D) primary cell culture models.

Dr. Manuel Peitsch is Chief Scientific Officer at PMI Research & Development. He leads the biomedical assessment of candidate modified risk tobacco products, consisting of preclinical toxicology, systems toxicology, and clinical study programs as well as regulatory affairs. Manuel (co)authored over 200 articles, book chapters, and patents in areas such as bioinformatics, text mining, and systems biology/toxicology. Manuel is a cofounder of the Swiss Institute of Bioinformatics and the chairman of its Board of Directors. Manuel holds a Ph.D. in biochemistry from the University of Lausanne and is an adjunct professor for bioinformatics at the University of Basel.

Dr. Julia Hoeng is Director of Systems Toxicology at PMI Research & Development where she leads the Systems Toxicology Program, covering a portfolio of projects from *in vitro*, *in vivo*, and *in silico* research for product testing. Julia obtained her Ph.D. and performed her postdoctoral research in Cambridge University and an M.S. in bioinformatics in the Georgia Institute of Technology, Atlanta, GA, USA. Julia has published numerous articles and book chapters highlighting the use of systems toxicology for risk assessment.

■ ACKNOWLEDGMENTS

We acknowledge Laura Ortega Torres and Stephanie Johne for maintenance of the organotypic cultures and for performing the AK and CYP activity assays, as well as the technical expertise of Rémi Dulize, Dariusz Peric, and Karine Baumer for the RNA sample processing and transcriptomics data generation. We thank also Sam Ansari for his support in the biobanking recording of the samples. We also acknowledge the technical expertise of Abdelkader Benyagoub, Camille Schilt, and Maude Mayer for the histological processing. We thank Stephanie Boué for her contribution in the preparation of the figures and Vincenzo Belcastro for support on the dataset submission to ArrayExpress. We also thank Grégory Vuillaume and Gilles Kreutzer for their contributions to the statistical evaluation of data from AK, secreted proinflammatory mediators, and CYP activity assays.

■ ABBREVIATIONS

3D, 3-dimensional;; 3Rs, replacement, reduction, and refinement; AK, adenylate kinase; ALI, air−liquid interface; BIF, biological impact factor; CEE, 6′-chloroethyl ether; CFA, cell fate; CPR, cell proliferation; CS, cigarette smoke; CSF, colony stimulating factor; CST, cellular stress; CXCL, chemokine (C-X-C motif) ligand; CYP, cytochrome P450; DEG, differentially expressed gene; DRA, dose range assessment; DRF, dose range finding; EDTA, ethylenediaminetetraacetic acid; FDR, false discovery rate; fRMA, frozen robust multiarray analysis; GSA, gene set analysis; H_2SO_4, sulfuric acid; HBD, human beta defensing; H&E, hematoxylin and eosin; IL, interleukin; IPN, inflammatory process network; ISO, international organization for standardization; KEGG, Kyoto encyclopedia of genes and genomes; *Limma*, linear models for microarray data; MAP, multianalyte profiling; MARLE, median absolute value relative log expression; miRNA, micro RNA; MMP, matrix metalloproteinase; MRTP, modified risk tobacco product; MTD, maximum tolerable dose; N, number; NFE2L2, nuclear factor (erythroid-derived 2)-like 2; NPA, network perturbation amplitude; NUSE, normalized-unscaled standard error; PAH, polycyclic aromatic hydrocarbon; PBS, phosphate-buffered saline; PFA, paraformaldehyde; RLE, relative log expression; SEM, standard error of the mean; SM, smoking machine; TCDD, 2,3,7,8-tetrachlorodibenzodioxin; TGFA, transforming growth factor alpha; THS, tobacco heating system; TJ, tight junction; TNF, tumor necrosis factor; w/v, weight/volume; VEGFA, vascular endothelial growth factor alpha

■ REFERENCES

(1) Sloan, P., Picardo, M., and Schor, S. L. (1991) The structure and function of oral mucosa. *Dental Update Publication 18*, 208−212.
(2) Andersson, G., Axell, T., and Larsson, A. (1989) Histologic changes associated with the use of loose and portion-bag packed Swedish moist snuff: a comparative study. *J. Oral Pathol. Med. 18*, 491−497.
(3) Lukandu, O. M., Neppelberg, E., Vintermyr, O. K., Johannessen, A. C., and Costea, D. E. (2010) Khat alters the phenotype of in vitro-reconstructed human oral mucosa. *J. Dent. Res. 89*, 270−275.
(4) Squier, C. A., and Kremer, M. J. (2001) Biology of oral mucosa and esophagus. *J. Natl. Cancer Inst. Monogr. 2001*, 7−15.
(5) Sasco, A. J., Secretan, M. B., and Straif, K. (2004) Tobacco smoking and cancer: a brief review of recent epidemiological evidence. *Lung Cancer 45* (Suppl. 2), S3−59.
(6) Warnakulasuriya, S., Dietrich, T., Bornstein, M. M., Casals Peidro, E., Preshaw, P. M., Walter, C., Wennstrom, J. L., and Bergstrom, J. (2010) Oral health risks of tobacco use and effects of cessation. *Int. Dent. J. 60*, 7−30.
(7) (2004) The 2004 United States Surgeon General's Report: The Health Consequences of Smoking. *NSW Public Health Bulletin*, Vol. *15*, p 107. https://www.cdc.gov/tobacco/data_statistics/sgr/2004/pdfs/executivesummary.pdf.
(8) Johnson, N. W., and Bain, C. A. (2000) Tobacco and oral disease. EU-Working Group on Tobacco and Oral Health. *Br. Dent. J. 189*, 200−206.
(9) Winn, D. M. (2001) Tobacco use and oral disease. *J. Dent. Educ. 65*, 306−312.
(10) Calsina, G., Ramon, J. M., and Echeverria, J. J. (2002) Effects of smoking on periodontal tissues. *J. Clin. Periodontol. 29*, 771−776.
(11) Moimaz, S. A., Zina, L. G., Saliba, O., and Garbin, C. A. (2009) Smoking and periodontal disease: clinical evidence for an association. *Oral Health Prev. Dent. 7*, 369−376.
(12) Gualerzi, A., Sciarabba, M., Tartaglia, G., Sforza, C., and Donetti, E. (2012) Acute effects of cigarette smoke on three-dimensional cultures of normal human oral mucosa. *Inhalation Toxicol. 24*, 382−389.
(13) Michcik, A., Cichorek, M., Daca, A., Chomik, P., Wojcik, S., Zawrocki, A., and Wlodarkiewicz, A. (2014) Tobacco smoking alters the number of oral epithelial cells with apoptotic features. *Folia Histochem. Cytobiol. 52*, 60−68.
(14) Sridhar, S., Schembri, F., Zeskind, J., Shah, V., Gustafson, A. M., Steiling, K., Liu, G., Dumas, Y. M., Zhang, X., Brody, J. S., Lenburg, M. E., and Spira, A. (2008) Smoking-induced gene expression changes in the bronchial airway are reflected in nasal and buccal epithelium. *BMC Genomics 9*, 259.
(15) Boyle, J. O., Gumus, Z. H., Kacker, A., Choksi, V. L., Bocker, J. M., Zhou, X. K., Yantiss, R. K., Hughes, D. B., Du, B., Judson, B. L.,

DOI: 10.1021/acs.chemrestox.6b00174
Chem. Res. Toxicol. 2016, 29, 1252−1269

Subbaramaiah, K., and Dannenberg, A. J. (2010) Effects of cigarette smoke on the human oral mucosal transcriptome. *Cancer Prev. Res. 3*, 266−278.
(16) Spira, A., Beane, J. E., Shah, V., Steiling, K., Liu, G., Schembri, F., Gilman, S., Dumas, Y. M., Calner, P., Sebastiani, P., Sridhar, S., Beamis, J., Lamb, C., Anderson, T., Gerry, N., Keane, J., Lenburg, M. E., and Brody, J. S. (2007) Airway epithelial gene expression in the diagnostic evaluation of smokers with suspect lung cancer. *Nat. Med. 13*, 361−366.
(17) Banerjee, A. G., Bhattacharyya, I., and Vishwanatha, J. K. (2005) Identification of genes and molecular pathways involved in the progression of premalignant oral epithelia. *Mol. Cancer Ther. 4*, 865−875.
(18) Khan, I., Kumar, N., Pant, I., Narra, S., and Kondaiah, P. (2012) Activation of TGF-beta pathway by areca nut constituents: a possible cause of oral submucous fibrosis. *PLoS One 7*, e51806.
(19) Noutomi, Y., Oga, A., Uchida, K., Okafuji, M., Ita, M., Kawauchi, S., Furuya, T., Ueyama, Y., and Sasaki, K. (2006) Comparative genomic hybridization reveals genetic progression of oral squamous cell carcinoma from dysplasia via two different tumourigenic pathways. *J. Pathol. 210*, 67−74.
(20) Proia, N. K., Paszkiewicz, G. M., Nasca, M. A., Franke, G. E., and Pauly, J. L. (2006) Smoking and smokeless tobacco-associated human buccal cell mutations and their association with oral cancer–a review. *Cancer Epidemiol., Biomarkers Prev. 15*, 1061−1077.
(21) Toruner, G. A., Ulger, C., Alkan, M., Galante, A. T., Rinaggio, J., Wilk, R., Tian, B., Soteropoulos, P., Hameed, M. R., Schwalb, M. N., and Dermody, J. J. (2004) Association between gene expression profile and tumor invasion in oral squamous cell carcinoma. *Cancer Genet. Cytogenet. 154*, 27−35.
(22) Zhang, L., and Rosin, M. P. (2001) Loss of heterozygosity: a potential tool in management of oral premalignant lesions? *J. Oral Pathol. Med. 30*, 513−520.
(23) Schlage, W. K., Iskandar, A. R., Kostadinova, R., Xiang, Y., Sewer, A., Majeed, S., Kuehn, D., Frentzel, S., Talikka, M., Geertz, M., Mathis, C., Ivanov, N., Hoeng, J., and Peitsch, M. C. (2014) In vitro systems toxicology approach to investigate the effects of repeated cigarette smoke exposure on human buccal and gingival organotypic epithelial tissue cultures. *Toxicol. Mech. Methods 24*, 470−487.
(24) BeruBe, K., Aufderheide, M., Breheny, D., Clothier, R., Combes, R., Duffin, R., Forbes, B., Gaca, M., Gray, A., Hall, I., Kelly, M., Lethem, M., Liebsch, M., Merolla, L., Morin, J. P., Seagrave, J., Swartz, M. A., Tetley, T. D., and Umachandran, M. (2009) In vitro models of inhalation toxicity and disease. The report of a FRAME workshop. *Altern. Lab. Anim. 37*, 89−141.
(25) Kimball, J. R., Nittayananta, W., Klausner, M., Chung, W. O., and Dale, B. A. (2006) Antimicrobial barrier of an in vitro oral epithelial model. *Arch. Oral Biol. 51*, 775−783.
(26) Klausner, M., Ayehunie, S., Breyfogle, B. A., Wertz, P. W., Bacca, L., and Kubilus, J. (2007) Organotypic human oral tissue models for toxicological studies. *Toxicol. In Vitro 21*, 938−949.
(27) Walle, T., Walle, U. K., Sedmera, D., and Klausner, M. (2006) Benzo[A]pyrene-induced oral carcinogenesis and chemoprevention: studies in bioengineered human tissue. *Drug Metab. Dispos. 34*, 346−350.
(28) Moyes, D. L., Runglall, M., Murciano, C., Shen, C., Nayar, D., Thavaraj, S., Kohli, A., Islam, A., Mora-Montes, H., Challacombe, S. J., and Naglik, J. R. (2010) A biphasic innate immune MAPK response discriminates between the yeast and hyphal forms of Candida albicans in epithelial cells. *Cell Host Microbe 8*, 225−235.
(29) Andrian, E., Grenier, D., and Rouabhia, M. (2004) In vitro models of tissue penetration and destruction by Porphyromonas gingivalis. *Infect. Immun. 72*, 4689−4698.
(30) Hansson, A., Bloor, B. K., Sarang, Z., Haig, Y., Morgan, P. R., Stark, H. J., Fusenig, N. E., Ekstrand, J., and Grafstrom, R. C. (2003) Analysis of proliferation, apoptosis and keratin expression in cultured normal and immortalized human buccal keratinocytes. *Eur. J. Oral Sci. 111*, 34−41.
(31) Mostefaoui, Y., Claveau, I., Ross, G., and Rouabhia, M. (2002) Tissue structure, and IL-1beta, IL-8, and TNF-alpha secretions after contact by engineered human oral mucosa with dentifrices. *J. Clin. Periodontol. 29*, 1035−1041.
(32) Xu, Q., Izumi, K., Tobita, T., Nakanishi, Y., and Feinberg, S. E. (2009) Constitutive release of cytokines by human oral keratinocytes in an organotypic culture. *J. Oral Maxillofac. Surg. 67*, 1256−1264.
(33) Brusevold, I. J., Soland, T. M., Khuu, C., Christoffersen, T., and Bryne, M. (2010) Nuclear and cytoplasmic expression of Met in oral squamous cell carcinoma and in an organotypic oral cancer model. *Eur. J. Oral Sci. 118*, 342−349.
(34) Pinnock, A., Murdoch, C., Moharamzadeh, K., Whawell, S., and Douglas, C. W. (2014) Characterisation and optimization of organotypic oral mucosal models to study Porphyromonas gingivalis invasion. *Microbes Infect. 16*, 310−319.
(35) Yadev, N. P., Murdoch, C., Saville, S. P., and Thornhill, M. H. (2011) Evaluation of tissue engineered models of the oral mucosa to investigate oral candidiasis. *Microb. Pathog. 50*, 278−285.
(36) Ceder, R., Merne, M., Staab, C. A., Nilsson, J. A., Hoog, J. O., Dressler, D., Engelhart, K., and Grafstrom, R. C. (2007) The application of normal, SV40 T-antigen-immortalised and tumour-derived oral keratinocytes, under serum-free conditions, to the study of the probability of cancer progression as a result of environmental exposure to chemicals. *Altern. Lab. Anim. 35*, 621−639.
(37) Hansson, A., Bloor, B. K., Haig, Y., Morgan, P. R., Ekstrand, J., and Grafstrom, R. C. (2001) Expression of keratins in normal, immortalized and malignant oral epithelia in organotypic culture. *Oral Oncol. 37*, 419−430.
(38) Manuppello, J. R., and Sullivan, K. M. (2015) Toxicity assessment of tobacco products in vitro. *Altern. Lab. Anim. 43*, 39−67.
(39) Balls, M. (2010) ATLA (Alternatives to Laboratory Animals): past, present and future. *Altern. Lab. Anim. 38*, 437−441.
(40) Tralau, T., Oelgeschlager, M., Gurtler, R., Heinemeyer, G., Herzler, M., Hofer, T., Itter, H., Kuhl, T., Lange, N., Lorenz, N., Muller-Graf, C., Pabel, U., Pirow, R., Ritz, V., Schafft, H., Schneider, H., Schulz, T., Schumacher, D., Zellmer, S., Fleur-Bol, G., Greiner, M., Lahrssen-Wiederholt, M., Lampen, A., Luch, A., Schonfelder, G., Solecki, R., Wittkowski, R., and Hensel, A. (2015) Regulatory toxicology in the twenty-first century: challenges, perspectives and possible solutions. *Arch. Toxicol. 89*, 823−850.
(41) Baker, M. (2011) Tissue models: a living system on a chip. *Nature 471*, 661−665.
(42) Hwa, A. J., Fry, R. C., Sivaraman, A., So, P. T., Samson, L. D., Stolz, D. B., and Griffith, L. G. (2007) Rat liver sinusoidal endothelial cells survive without exogenous VEGF in 3D perfused co-cultures with hepatocytes. *FASEB J. 21*, 2564−2579.
(43) Tralau, T., and Luch, A. (2012) Drug-mediated toxicity: illuminating the 'bad' in the test tube by means of cellular assays? *Trends Pharmacol. Sci. 33*, 353−364.
(44) Knudsen, T. B., Keller, D. A., Sander, M., Carney, E. W., Doerrer, N. G., Eaton, D. L., Fitzpatrick, S. C., Hastings, K. L., Mendrick, D. L., Tice, R. R., Watkins, P. B., and Whelan, M. (2015) FutureTox II: in vitro data and in silico models for predictive toxicology. *Toxicol. Sci. 143*, 256−267.
(45) Modified Risk TobaccoProduct Applications: Draft Guidance, http://www.fda.gov/downloads/TobaccoProducts/GuidanceComplianceRegulatoryInformation/UCM297751.pdf.
(46) Stratton, K., Shetty, P., Wallace, R., and Bondurant, S. (2001) Clearing the smoke: the science base for tobacco harm reduction–executive summary. *Tob. Control 10*, 189−195.
(47) International Organization for Standardization (1999) Tobacco and Tobacco Products: Atmosphere for Conditioning and Testing, Switzerland, http://www.iso.org/iso/home/store/catalogue_tc/catalogue_detail.htm?csnumber=28324.
(48) Health Canada (1999) *Determination of Tar, Water, Nicotine and Carbon Monoxide in Mainstream Tobacco Smoke. Health Canada Test Method T-11.* http://edge.rit.edu/edge/P10056/public/Health%20Canada%20Nicotine.
(49) Majeed, S., Frentzel, S., Wagner, S., Kuehn, D., Leroy, P., Guy, P. A., Knorr, A., Hoeng, J., and Peitsch, M. C. (2014) Characterization of

DOI: 10.1021/acs.chemrestox.6b00174
Chem. Res. Toxicol. 2016, 29, 1252−1269

the Vitrocell(R) 24/48 in vitro aerosol exposure system using mainstream cigarette smoke. *Chem. Cent. J. 8*, 62.
(50) Hoeng, J., Talikka, M., Martin, F., Sewer, A., Yang, X., Iskandar, A., Schlage, W. K., and Peitsch, M. C. (2014) Case study: the role of mechanistic network models in systems toxicology. *Drug Discovery Today 19*, 183−192.
(51) Boue, S., Talikka, M., Westra, J. W., Hayes, W., Di Fabio, A., Park, J., Schlage, W. K., Sewer, A., Fields, B., Ansari, S., Martin, F., Veljkovic, E., Kenney, R., Peitsch, M. C., and Hoeng, J. (2015) Causal biological network database: a comprehensive platform of causal biological network models focused on the pulmonary and vascular systems. *Database 2015*, bav030.
(52) Martin, F., Sewer, A., Talikka, M., Xiang, Y., Hoeng, J., and Peitsch, M. C. (2014) Quantification of biological network perturbations for mechanistic insight and diagnostics using two-layer causal models. *BMC Bioinf. 15*, 238.
(53) Thomson, T. M., Sewer, A., Martin, F., Belcastro, V., Frushour, B. P., Gebel, S., Park, J., Schlage, W. K., Talikka, M., Vasilyev, D. M., Westra, J. W., Hoeng, J., and Peitsch, M. C. (2013) Quantitative assessment of biological impact using transcriptomic data and mechanistic network models. *Toxicol. Appl. Pharmacol. 272*, 863−878.
(54) Gentleman, R. C., Carey, V. J., Bates, D. M., Bolstad, B., Dettling, M., Dudoit, S., Ellis, B., Gautier, L., Ge, Y., Gentry, J., Hornik, K., Hothorn, T., Huber, W., Iacus, S., Irizarry, R., Leisch, F., Li, C., Maechler, M., Rossini, A. J., Sawitzki, G., Smith, C., Smyth, G., Tierney, L., Yang, J. Y., and Zhang, J. (2004) Bioconductor: open software development for computational biology and bioinformatics. *Genome Biol. 5*, R80.
(55) Davis, M. A., Eldridge, S., and Louden, C. (2013) Biomarkers: Discovery, Qualification and Application, in *Haschek and Rousseaux's Handbook of Toxicologic Pathology* (Wallig, W. M. H. G. R. A., Ed.) 3rd ed., pp 317−352, Chapter 10, Academic Press, Boston, MA.
(56) van Roy, F., and Berx, G. (2008) The cell-cell adhesion molecule E-cadherin. *Cell. Mol. Life Sci. 65*, 3756−3788.
(57) Tsang, S. M., Brown, L., Lin, K., Liu, L., Piper, K., O'Toole, E. A., Grose, R., Hart, I. R., Garrod, D. R., Fortune, F., and Wan, H. (2012) Non-junctional human desmoglein 3 acts as an upstream regulator of Src in E-cadherin adhesion, a pathway possibly involved in the pathogenesis of pemphigus vulgaris. *J. Pathol. 227*, 81−93.
(58) Hukkanen, J., Pelkonen, O., Hakkola, J., and Raunio, H. (2002) Expression and regulation of xenobiotic-metabolizing cytochrome P450 (CYP) enzymes in human lung. *Crit. Rev. Toxicol. 32*, 391−411.
(59) Vondracek, M., Xi, Z., Larsson, P., Baker, V., Mace, K., Pfeifer, A., Tjalve, H., Donato, M. T., Gomez-Lechon, M. J., and Grafstrom, R. C. (2001) Cytochrome P450 expression and related metabolism in human buccal mucosa. *Carcinogenesis 22*, 481−488.
(60) Boué, S., Talikka, M., Westra, J. W., Hayes, W., Di Fabio, A., Park, J., Schlage, W. K., Sewer, A., Fields, B., Ansari, S., Martin, F., Veljkovic, E., Kenney, R., Peitsch, M. C., and Hoeng, J. (2015) Causal biological network database: a comprehensive platform of causal biological network models focused on the pulmonary and vascular systems. *Database 2015*, bav030.
(61) Talikka, M., Kostadinova, R., Xiang, Y., Mathis, C., Sewer, A., Majeed, S., Kuehn, D., Frentzel, S., Merg, C., Geertz, M., Martin, F., Ivanov, N. V., Peitsch, M. C., and Hoeng, J. (2014) The response of human nasal and bronchial organotypic tissue cultures to repeated whole cigarette smoke exposure. *Int. J. Toxicol. 33*, 506−517.
(62) Donetti, E., Gualerzi, A., Bedoni, M., Volpari, T., Sciarabba, M., Tartaglia, G., and Sforza, C. (2010) Desmoglein 3 and keratin 10 expressions are reduced by chronic exposure to cigarette smoke in human keratinised oral mucosa explants. *Arch. Oral Biol. 55*, 815−823.
(63) Su, L., Morgan, P. R., Thomas, J. A., and Lane, E. B. (1993) Expression of keratin 14 and 19 mRNA and protein in normal oral epithelia, hairy leukoplakia, tongue biting and white sponge nevus. *J. Oral Pathol. Med. 22*, 183−189.
(64) Yoshizawa, M., Koyama, T., Kojima, T., Kato, H., Ono, Y., and Saito, C. (2012) Keratinocytes of tissue-engineered human oral mucosa promote re-epithelialization after intraoral grafting in athymic mice. *J. Oral Maxillofac. Surg. 70*, 1199−1214.
(65) Bloor, B. K., Su, L., Shirlaw, P. J., and Morgan, P. R. (1998) Gene expression of differentiation-specific keratins (4/13 and 1/10) in normal human buccal mucosa. *Lab. Invest. 78*, 787−795.
(66) Mahoney, M. G., Hu, Y., Brennan, D., Bazzi, H., Christiano, A. M., and Wahl, J. K., 3rd (2006) Delineation of diversified desmoglein distribution in stratified squamous epithelia: implications in diseases. *Exp. Dermatol. 15*, 101−109.
(67) Mirowsk, G. W., Lozada-Nur, F., Dekker, N. P., MacPhail, L. A., and Regezi, J. A. (1996) Altered expression of epithelial integrins and extracellular matrix receptors in oral erythema multiforme. *J. Cutaneous Pathol. 23*, 473−478.
(68) Kose, O., Lalli, A., Kutulola, A. O., Odell, E. W., and Waseem, A. (2007) Changes in the expression of stem cell markers in oral lichen planus and hyperkeratotic lesions. *J. Oral Sci. 49*, 133−139.
(69) Garrod, D., and Chidgey, M. (2008) Desmosome structure, composition and function. *Biochim. Biophys. Acta, Biomembr. 1778*, 572−587.
(70) Takai, Y., Irie, K., Shimizu, K., Sakisaka, T., and Ikeda, W. (2003) Nectins and nectin-like molecules: roles in cell adhesion, migration, and polarization. *Cancer Sci. 94*, 655−667.
(71) Okabe, N., Ozaki-Kuroda, K., Nakanishi, H., Shimizu, K., and Takai, Y. (2004) Expression patterns of nectins and afadin during epithelial remodeling in the mouse embryo. *Dev. Dyn. 230*, 174−186.
(72) Watt, F. M., Estrach, S., and Ambler, C. A. (2008) Epidermal Notch signalling: differentiation, cancer and adhesion. *Curr. Opin. Cell Biol. 20*, 171−179.
(73) Findley, M. K., and Koval, M. (2009) Regulation and roles for claudin-family tight junction proteins. *IUBMB Life 61*, 431−437.
(74) Furuse, M., Fujita, K., Hiiragi, T., Fujimoto, K., and Tsukita, S. (1998) Claudin-1 and −2: novel integral membrane proteins localizing at tight junctions with no sequence similarity to occludin. *J. Cell Biol. 141*, 1539−1550.
(75) Pritchard, C. C., Cheng, H. H., and Tewari, M. (2012) MicroRNA profiling: approaches and considerations. *Nat. Rev. Genet. 13*, 358−369.
(76) Sheldon, L. S., and Cohen Hubal, E. A. (2009) Exposure as part of a systems approach for assessing risk. *Environ. Health Perspect. 117*, 119−1194.
(77) Berg, N., De Wever, B., Fuchs, H. W., Gaca, M., Krul, C., and Roggen, E. L. (2011) Toxicology in the 21st century–working our way towards a visionary reality. *Toxicol. In Vitro 25*, 874−881.
(78) Rovida, C., Asakura, S., Daneshian, M., Hofman-Huether, H., Leist, M., Meunier, L., Reif, D., Rossi, A., Schmutz, M., Valentin, J. P., Zurlo, J., and Hartung, T. (2015) Toxicity testing in the 21st century beyond environmental chemicals. *ALTEX 32*, 171−181.
(79) Mathis, C., Poussin, C., Weisensee, D., Gebel, S., Hengstermann, A., Sewer, A., Belcastro, V., Xiang, Y., Ansari, S., Wagner, S., Hoeng, J., and Peitsch, M. C. (2013) Human bronchial epithelial cells exposed in vitro to cigarette smoke at the air-liquid interface resemble bronchial epithelium from human smokers. *Am. J. Physiol. Lung Cell Mol. Physiol. 304*, L489−503.
(80) Iskandar, A. R., Xiang, Y., Frentzel, S., Talikka, M., Leroy, P., Kuehn, D., Guedj, E., Martin, F., Mathis, C., Ivanov, N. V., Peitsch, M. C., and Hoeng, J. (2015) Impact Assessment of Cigarette Smoke Exposure on Organotypic Bronchial Epithelial Tissue Cultures: A Comparison of Mono-Culture and Coculture Model Containing Fibroblasts. *Toxicol. Sci. 147*, 207−221.
(81) Chinnathambi, S., Tomanek-Chalkley, A., Ludwig, N., King, E., DeWaard, R., Johnson, G., Wertz, P. W., and Bickenbach, J. R. (2003) Recapitulation of oral mucosal tissues in long-term organotypic culture. *Anat. Rec. 270A*, 162−174.
(82) Kogel, U., Schlage, W. K., Martin, F., Xiang, Y., Ansari, S., Leroy, P., Vanscheeuwijck, P., Gebel, S., Buettner, A., Wyss, C., Esposito, M., Hoeng, J., and Peitsch, M. C. (2014) A 28-day rat inhalation study with an integrated molecular toxicology endpoint demonstrates reduced exposure effects for a prototypic modified risk tobacco product compared with conventional cigarettes. *Food Chem. Toxicol. 68*, 204−217.
(83) Phillips, B., Esposito, M., Verbeeck, J., Boue, S., Iskandar, A., Vuillaume, G., Leroy, P., Krishnan, S., Kogel, U., Utan, A., Schlage, W. K.,

DOI: 10.1021/acs.chemrestox.6b00174
Chem. Res. Toxicol. 2016, 29, 1252−1269

Bera, M., Veljkovic, E., Hoeng, J., Peitsch, M. C., and Vanscheeuwijck, P. (2015) Toxicity of aerosols of nicotine and pyruvic acid (separate and combined) in Sprague-Dawley rats in a 28-day OECD 412 inhalation study and assessment of systems toxicology. *Inhalation Toxicol. 27*, 405−431.
(84) Sidorova, Y. A., and Grishanova, A. Y. (2005) Inhibitory effect of alpha-tocopherol on benzo(a)pyrene-induced CYPA1 activity in rat liver. *Bull. Exp. Biol. Med. 140*, 517−520.
(85) Amara, I. E., Anwar-Mohamed, A., and El-Kadi, A. O. (2010) Mercury modulates the CYP1A1 at transcriptional and posttranslational levels in human hepatoma HepG2 cells. *Toxicol. Lett. 199*, 225−233.
(86) Anwar-Mohamed, A., Klotz, L. O., and El-Kadi, A. O. (2012) Inhibition of heme oxygenase-1 partially reverses the arsenite-mediated decrease of CYP1A1, CYP1A2, CYP3A23, and CYP3A2 catalytic activity in isolated rat hepatocytes. *Drug Metab. Dispos. 40*, 504−514.
(87) Korashy, H. M., and El-Kadi, A. O. (2012) Transcriptional and posttranslational mechanisms modulating the expression of the cytochrome P450 1A1 gene by lead in HepG2 cells: a role of heme oxygenase. *Toxicology 291*, 113−121.
(88) Park, J. W., Reed, J. R., and Backes, W. L. (2015) The Localization of Cytochrome P450s CYP1A1 and CYP1A2 into Different Lipid Microdomains Is Governed by Their N-terminal and Internal Protein Regions. *J. Biol. Chem. 290*, 29449−29460.
(89) Burke, R. S., Somasuntharam, I., Rearden, P., Brown, D., Deshmukh, S. V., DiPietro, M. A., DiMuzio, J., Eisenhandler, R., Fauty, S. E., Gibson, C., Gindy, M. E., Hamilton, K. A., Knemeyer, I., Koeplinger, K. A., Kwon, H. W., Lifsted, T. Q., Menzel, K., Patel, M., Pudvah, N., Rudd, D. J., Seitzer, J., Strapps, W. R., Prueksaritanont, T., Thompson, C. D., Hochman, J. H., and Carr, B. A. (2014) siRNA-mediated knockdown of P450 oxidoreductase in rats: a tool to reduce metabolism by CYPs and increase exposure of high clearance compounds. *Pharm. Res. 31*, 3445−3460.
(90) Fang, C., and Zhang, Q. Y. (2010) The role of small-intestinal P450 enzymes in protection against systemic exposure of orally administered benzo[a]pyrene. *J. Pharmacol. Exp. Ther. 334*, 156−163.
(91) Lee, C., Ding, X., and Riddick, D. S. (2013) The role of cytochrome P450-dependent metabolism in the regulation of mouse hepatic growth hormone signaling components and target genes by 3-methylcholanthrene. *Drug Metab. Dispos. 41*, 457−465.
(92) Mishin, V., Heck, D. E., Laskin, D. L., and Laskin, J. D. (2014) Human recombinant cytochrome P450 enzymes display distinct hydrogen peroxide generating activities during substrate independent NADPH oxidase reactions. *Toxicol. Sci. 141*, 344−352.
(93) Zhang, Q. Y., Fang, C., Zhang, J., Dunbar, D., Kaminsky, L., and Ding, X. (2009) An intestinal epithelium-specific cytochrome P450 (P450) reductase-knockout mouse model: direct evidence for a role of intestinal p450s in first-pass clearance of oral nifedipine. *Drug Metab. Dispos. 37*, 651−657.
(94) Marohnic, C. C., Huber Iii, W. J., Patrick Connick, J., Reed, J. R., McCammon, K., Panda, S. P., Martasek, P., Backes, W. L., and Masters, B. S. (2011) Mutations of human cytochrome P450 reductase differentially modulate heme oxygenase-1 activity and oligomerization. *Arch. Biochem. Biophys. 513*, 42−50.
(95) Pandey, A. V., Fluck, C. E., and Mullis, P. E. (2010) Altered heme catabolism by heme oxygenase-1 caused by mutations in human NADPH cytochrome P450 reductase. *Biochem. Biophys. Res. Commun. 400*, 374−378.
(96) Li, D. N., Pritchard, M. P., Hanlon, S. P., Burchell, B., Wolf, C. R., and Friedberg, T. (1999) Competition between cytochrome P-450 isozymes for NADPH-cytochrome P-450 oxidoreductase affects drug metabolism. *J. Pharmacol. Exp. Ther. 289*, 661−667.
(97) Watanabe, N., and Kobayashi, Y. (1994) Selective release of a processed form of interleukin 1 alpha. *Cytokine 6*, 597−601.
(98) Chakraborti, S., Mandal, M., Das, S., Mandal, A., and Chakraborti, T. (2003) Regulation of matrix metalloproteinases: an overview. *Mol. Cell. Biochem. 253*, 269−285.
(99) Herlofson, B. B., and Barkvoll, P. (1996) Oral mucosal desquamation caused by two toothpaste detergents in an experimental model. *Eur. J. Oral Sci. 104*, 21−26.
(100) Muller, W., and Schroeder, H. E. (1980) Differentiation of the epithelium of the human hard palate. *Cell Tissue Res. 209*, 295−313.
(101) Plackova, A., and Skach, M. (1975) [Fine structural study of keratinization of the filiform papillae in the tongue in humans]. *Z. Mikrosk.-Anat. Forsch. 89*, 305−318.
(102) Singh, B. B., Schuster, G. S., Merchant, V. A., and Michelich, V. J. (1979) Ultrastructural and autoradiographic observations of hamster cheek pouch epithelium grown in vitro. *In Vitro 15*, 865−872.
(103) Orellana-Bustos, A. I., Espinoza-Santander, I. L., Franco-Martinez, M. E., Lobos-James-Freyre, N., and Ortega-Pinto, A. V. (2004) Evaluation of keratinization and AgNORs count in exfoliative cytology of normal oral mucosa from smokers and non-smokers. *Med. Oral 9*, 197−203.
(104) Johnson, N. (2001) Tobacco use and oral cancer: a global perspective. *J. Dent. Educ. 65*, 328−339.
(105) Coppe, J. P., Boysen, M., Sun, C. H., Wong, B. J., Kang, M. K., Park, N. H., Desprez, P. Y., Campisi, J., and Krtolica, A. (2008) A role for fibroblasts in mediating the effects of tobacco-induced epithelial cell growth and invasion. *Mol. Cancer Res. 6*, 1085−1098.

DOI: 10.1021/acs.chemrestox.6b00174
Chem. Res. Toxicol. 2016, 29, 1252−1269